ACS OMEGA

Open Access

http://pubs.acs.org/journal/acsodf

Article

Modified Amber Particles as a Stabilizer to Construct Oil-in-Water Pickering Emulsions for Improved Thermal Stability of *Acorus tatarinowii* Essential Oil

Zhonghuan Qu, Yajun Shi, Xiaofei Zhang, Fei Luan, Dongyan Guo, Bingtao Zhai, Jing Sun, Dingkun Zhang, Junbo Zou,* and Maomao Zhu*

Cite This: *ACS Omega* 2024, 9, 20773−20790

Read Online

ACCESS | Metrics & More | Article Recommendations | Supporting Information

ABSTRACT: Lingzhu Pulvis is a classic formulation for treating febrile convulsions in children. However, *Acorus tatarinowii* essential oil (AT-EO) in this prescription is prone to volatilization and oxidation, compromising the efficacy and quality control of this formulation. Herein, based on the concept of "combination of medicine and adjuvant", Pickering emulsion technology was applied to enhance the stability of AT-EO using modified amber as a stabilizer. Amber was a resinous medicinal powder in Lingzhu Pulvis and was modified into a suitable stabilizer for Pickering emulsion through surface modification. A thermal stability study indicated that Pickering emulsion, stabilized by modified amber, exhibited a higher retention rate of AT-EO and lower levels of peroxide value and malondialdehyde content compared to those of the pure AT-EO group after heat treatment at 40 °C for 1, 3, and 8 h. Additionally, component analysis in content and composition revealed that the volatile components of AT-EO in the Pickering emulsion were more stable during the thermal treatment process. This study convincingly illustrates the potential of a Pickering emulsion stabilized with modified medicinal powders to improve the thermal stability of the essential oil.

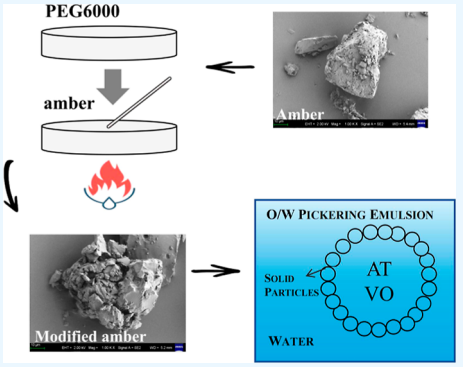

1. INTRODUCTION

Essential oils in Chinese medicine contain abundant active ingredients and demonstrate significant pharmacological activities in the nervous system, cardiovascular system, respiratory system, gastrointestinal system, etc.[1−5] These oils also exhibit noteworthy antibacterial/antifungal, antiviral, anti-inflammatory, and anticancer effects.[6] However, essential oils are prone to volatilization and oxidation when exposed to light, oxygen, and high temperatures. This can lead to changes in the content and composition of essential oils[7] and pose new challenges for the clinical use of essential oils.[8] Lingzhu Pulvis, a traditional Chinese medicine prescription, is composed of saigae tataricae cornu, bovis calculus artifactus, pearl powder, cinnabaris, the extracts of bombyx batryticatus and arisaema cum bile, amber, and AT-EO. It is primarily used for the treatment of febrile convulsions in children.[9] AT-EO in Lingzhu Pulvis usually adopts a spray form during preparation, which can easily evaporate during storage and usage. Therefore, there is an urgent need to enhance the stability of AT-EO in the Lingzhu Pulvis (see Scheme 1).

Pickering emulsions represent an innovative class of emulsions in which solid particles are employed to act as stabilizers. These stabilizing particles can range from inorganic materials such as silica, alumina, and clay,[10−12] to natural substances like starch, proteins, and their modified derivatives[13−15] and extend to synthetic materials like polymers.[16] The use of solid particles in Pickering emulsions circumvents the need for conventional surfactants, thus avoiding potential allergic reactions or irritations caused by surfactants. Meanwhile, they are characterized by their remarkable stability, low toxicity, and superior biocompatibility,[17] Pickering emulsions have rapidly gained popularity and utility across various industries, including the food, cosmetics, and pharmaceutical sectors.[16,18]

The "Combination of Medicine and Adjuvant" is an important principle in the utilization of excipients and is widely applied in Chinese medicine preparations.[19,20] Drawing upon this principle and the goal of enhancing the stability of volatile oil, our team aims to prepare a Pickering emulsion of AT-EO using the medicinal powders in Lingzhu Pulvis as stabilizers to bolster the stability of AT-EO. In a previous study, we investigated the emulsification effect of medicinal powders in Lingzhu Pulvis and found that pearl powder was a suitable O/W-type stabilizer. Subsequent studies have

Received: October 16, 2023
Revised: April 21, 2024
Accepted: April 23, 2024
Published: May 4, 2024

Scheme 1. Research Strategy Diagram for Enhancing the Stability of Volatile Oil with Pickering Emulsion Stabilized by Modified Suitable Stabilizer Based on the Concept of "Combination of Medicine and Adjuvant". (A) Diverse Types of Medicinal Powders with Strong Representativeness in Lingzhu Pulvis. (B) Emulsification Effect of Medicinal Powders in Lingzhu Pulvis. (C) Design of Suitable Stabilizers by Particle Design Technology. (D) Pickering Emulsion Stabilized by Modified Suitable Stabilizer to Enhance Volatile Oil Stability

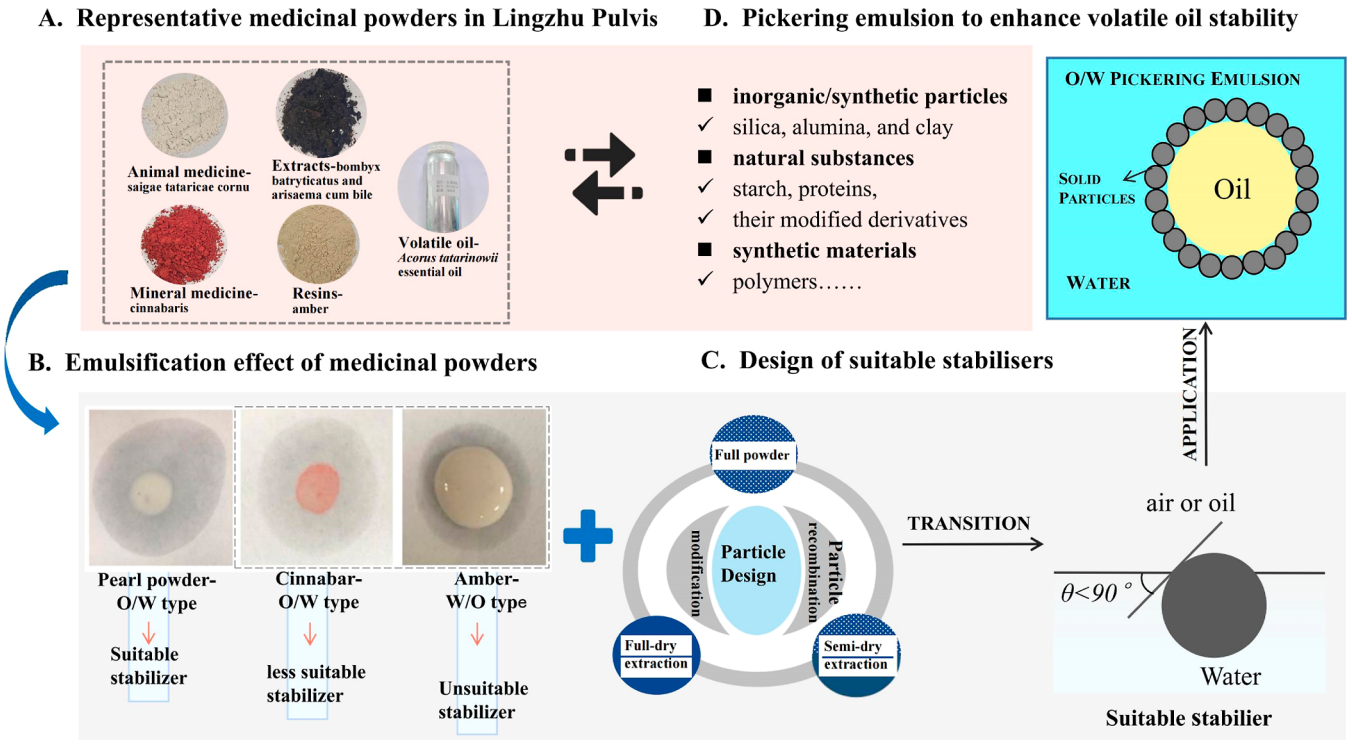

indicated that the Pickering emulsion stabilized by pearl powder could improve volatilization and oxidation of AT-EO.[21−23] Contrastingly, amber, owing to its poor water solubility was proved to be a unsuitable O/W-type stabilizer.[21]

To address the issue of the unsuitable medicinal powders in Lingzhu Pulvis as stabilizers for Pickering emulsion and further expand the depth of research on particle design technology,[24,25] including surface modification and particle recombination techniques, can be utilized as innovative methods to design suitable particles. Chen Qiuhong and his team[26] have successfully applied the octenyl succinic anhydride for the surface modification of cellulose nanocrystals (CNCs), which ameliorates the hydrophilic properties and improves the emulsifying capacity of CNCs, enabling the modified CNCs to be employed in crafting Pickering high internal phase emulsions. Similarly, Andreia Ribeiro et al.[27] utilize sodium oleate to modify the surface of nanohydroxyapatite (n-HAp) particles, the wettability of modified n-HAp particles shows a dependence on the content of sodium oleate. In summary, related modification methods can be employed to improve the surface properties of solid powders, enabling them to function as effective stabilizers for the Pickering emulsion. In this study, we aim to modify amber powders into a suitable stabilizer and further examine the stability of AT-EO in Pickering emulsion stabilized by modified amber under a thermal environment. This research will provide valuable insights into improving the stability of essential oils in solid preparations.

2. MATERIALS AND METHODS

2.1. Materials. Amber was provided by the Lei Yun Shang Pharmaceutical Group Co., Ltd. (Suzhou, China). AT-EO was pure *Acorus tatarinowii* essential oil and was bought from Xian Deshengyuan Biotechnology Co., Ltd. (Xian, China). PEG6000, Sudan III, and ethylenediaminetetraacetic acid disodium salt were purchased from Tianjin Kemiou Chemical Reagent Co., Ltd. (Tianjin, China). Trichloroacetic acid was acquired from the Tianjin Damao Chemical Reagent Factory (Tianjin, China). Methylene Blue, 2-thiobarbituric acid (AR, 98.5%), and 1,1,3,3-tetraethoxypropane (BR, 95%) were purchased from Shanghai Yuan Ye Bio-Technology Co., Ltd. (Shanghai, China). *n*-Docosane (99.6%) was acquired from LGC Labor GmbH (Augsburg, Germany). Water was pure water, and all other reagents were analytical grade.

2.2. Preparation and Characterization of Modified Amber. *2.2.1. Single-Factor Experiment.* To explore the effects of various factors on the emulsification properties of modified amber particles, a single-factor experiment was conducted, which was established on the electric heating jacket (Beijing Keweiyongxing Instrument Co., Ltd.) voltage of 150 V, modification time of 5 min, modification adjuvant of PEG6000, and ratio of adjuvant to amber of 1:1. The evaluation parameter was the height of the emulsion layer after centrifugation (4000 rpm for 15 min). This experiment inspected the influences of four factors at different levels, including the voltage of the electric heating jacket (100 and 150 V), modification time (3, 4, 5, 6 min), modification adjuvant (PEG400, PEG2000, PEG4000, and PEG6000), and the ratio of PEG6000 to amber (ratios of 1:4, 2:4, 3:4, and 4:4).

2.2.2. Characterization of Modified Amber. 2.2.2.1. Surface Free Energy Determination Model. The most commonly used Owens−Wendt−Rabel−Kaelble model[28] was chosen to

https://doi.org/10.1021/acsomega.3c08110
ACS Omega 2024, 9, 20773−20790

examine the surface free energy and the polar and nonpolar components of modified amber and amber samples, based on the method of Qin et al.[29] The test liquids were water, methanol, and ethylene glycol, and the surface free energy and its components of the model liquids used in this experiment are shown in Table 1. The calculation formula for the surface free energy refers to eq 1, and the method for contact angle (θ)[9] is as follows: 0.2 g of modified amber and amber powder was weighed and then compressed into sheets at the set pressure of 6 N with a powder press machine. The diameter and thickness of the sheet was measured, and it was secured on the sample stage using a clamp. The sample cup was filled with two-thirds the volume of water, the sample stage was gradually raised until the sheet was approximately 0.5 cm away from the liquid surface, and the contact angle was measured using K100C-KRUSS fully automatic surface tension and contact angle tester (KRUSS, Germany).

Table 1. Surface Free Energy of Model Liquids and Its Dispersive and Polar Components

model liquid	γ_L (mJ/m^2)	γ_L^d (mJ/m^2)	γ_L^p (mJ/m^2)
water	72.8	21.8	51
methanol	22.7	16	6.7
ethylene glycol	48	29	19

$$\gamma_L(1 + \cos\theta)/2(\gamma_L^d)^{1/2} = (\gamma_S^d)^{1/2} + (\gamma_S^p)^{1/2}(\gamma_L^p/\gamma_L^d)^{1/2} \quad (1)$$

where γ_L, γ_L^d, and γ_L^p are the total, dispersive, and polar parts of liquid surface free energies (mJ/m^2); γ_S^d and γ_S^p are the dispersive and polar components of solid surface free energy (mJ/m^2), respectively.

Linear analysis in terms of $\gamma_L(1 + \cos\theta)/2(\gamma_L^d)^{1/2}$ against $(\gamma_L^p/\gamma_L^d)^{1/2}$, fit a linear equation and calculate its correlation coefficient, R-squared (R^2). The slope and intercept correspond to the polar part $(\gamma_S^p)^{1/2}$ and the dispersive part $(\gamma_S^d)^{1/2}$ of the surface free energy of samples, respectively. The solid surface free energy γ_S is equal to the sum of γ_S^p and γ_S^d.

2.2.2.2. Particle Wettability. The air−water contact angle (θ_{aw}) was used to evaluate the wettability of amber and modified amber[27,30] conducted by an optical contact angle measurement instrument (LSA100, LAUDA Scientific, Germany). Amber and modified amber samples were pressed into circular tablets with a thickness of 5 mm and a diameter of 20 mm. The θ_{aw} was measured by taking an image of the water droplet on the surface of the sample tablet with a high-speed video camera connected to the apparatus. The contact angle values between the water droplet and the compressed tablet (left and right) were then automatically calculated with SurfaceMeter software.

2.2.2.3. Fourier Transform Infrared Spectroscopy. Fourier transform infrared spectroscopy (FT-IR) was performed using the KBr pellet method on a TENSOR-27 Fourier Transform Infrared Spectrometer (Bruker, Germany), according to the method described by Chen et al.[31] A suitable amount of amber, PEG6000, a physical mixture of PEG6000 and amber (the ratio was 1:2), and modified amber particles were scoped, mixed thoroughly with dried potassium bromide at the ratio of 1:100, and ground into a fine powder. Then, the mixture was pressed into a transparent slice using a powder press machine at a set pressure of 8 N, and the infrared spectrum of the samples was measured in the scanning range of 4000 to 400 cm^{-1}.

2.2.2.4. Scanning Electron Microscopy and Energy Dispersive X-ray Spectroscopy. Zeiss GeminiSEM360 (Carl Zeiss) was used to check the morphology and surface elemental of amber, PEG6000, and modified amber, referring to the method described by Huang et al.[32] Specifically, a small number of samples were adhered to the conductive adhesive, followed by coating with Au. The conductive adhesive was secured onto the sample holder, and the door of the sample chamber was closed and vacuumed. Then, the position of the conductive adhesive and magnification were adjusted, an electron beam was emitted onto the surface of the samples, and the surface morphology of the samples. Elemental analysis involved scanning surface regions of the sample with an electron beam to obtain the proportions of elements on the surface of the specimen.

2.3. Preparation and Characterization of Pickering Emulsion. *2.3.1. Single-Factor Experiment.* To evaluate the effects of different factors on Pickering emulsions prepared using an IKA T18 digital high-speed disperser (Shanghai Tusen Vision Technology Co., Ltd.), based on the added amount of modified amber particles of 5 μg/mL, a volume fraction of AT-EO of 50%, a shear speed of 13,000 rpm, and a shear time of 2 min, a single-factor experiment was conducted. The evaluation parameters were the emulsion stability index (ESI) and the height of the emulsion layer after centrifugation (4000 rpm for 15 min). The experiment investigated four factors, including the added amount of modified amber particles (2.5, 5, 7.5, 10, 12.5, 15, 17.5, 20, 22.5, and 25 μg/mL), the volume fraction of AT-EO (45, 50, 55, 60, 65, 70, 75, 80, and 85%), shear rate (5000, 7000, 9000, 11,000, 13,000, and 15,000 rpm), and shear time (1, 2, 3, and 4 min).

2.3.2. Measurement of ESI. The ESI of Pickering emulsions was assessed using turbidimetry.[33,34] A 30 μL freshly prepared Pickering emulsion was taken 0.5 cm from the bottom of the beaker into a 10 mL volumetric flask and dispersed with a 0.1% SDS solution. Absorbance (A_0) of the sample solution was measured at 500 nm using a UV-6100 DOUBLE BEAM UV−visible Spectrophotometer (Shanghai Mapuda Instrument Co., Ltd.) with 0.1% SDS solution as the blank. After 10 min of stewing, another 30 μL aliquots were obtained from the bottom of the beaker and dispersed with 10 mL of a 0.1% SDS solution. Absorbance (A_{10}) was measured at 500 nm as previously. The ESI of the emulsion samples was calculated as follows

$$\text{ESI}\,\% = \frac{A_{10}}{A_0} \times 100\% \quad (2)$$

where A_0 and A_{10} are the absorbances of emulsion samples at 0 and 10 min, respectively.

2.3.3. Characterization of Pickering Emulsion. 2.3.3.1. Emulsion Type. The Sudan III and methylene blue staining experiment was applied to examine the emulsion type. An appropriate amount of Pickering emulsion was taken, along with equal volumes of 1% methylene blue water solution and 0.5% Sudan III 70% ethanol solution. Shook well and allowed to stand for 10 min to ensure the dyeing effect. Then, a small amount of stained emulsion was dropped on the clean glass slide, the cover slide was placed at a certain angle with the glass slide, and the cover slide was slowly lowered to avoid the formation of bubbles. The glass slide was secured onto the

https://doi.org/10.1021/acsomega.3c08110
ACS Omega 2024, 9, 20773−20790

microscope stage, the aperture and focus were adjusted, and then the staining of Pickering emulsion was observed under a 10× objective lens using a N-300 M biological microscope.

2.3.3.2. Droplet Size. Microtrac S35000 Laser Particle Sizer (DKSH Commercial (China) Ltd.) was utilized for measuring the droplet size of Pickering emulsion under the wet method. Water served as the dispersing medium, an appropriate amount of Pickering emulsion samples was added until the red sample addition display bar was within the green range, and the measurement was performed.

2.3.3.3. Near-Infrared Spectrum. The ANTIRIS II Fourier Transform Near Infrared Spectrometer (Thermo Fisher Scientific (USA)) was employed to measure the near-infrared spectrum (NIRS) of AT-EO, modified amber suspension (7.5 μg/mL), and Pickering emulsion samples, according to the method conducted by Peng et al.[22] The samples were adjusted to the accompanying quartz sample cup and ensured that the cup bottom was fully submerged. The NIRS spectrum was acquired at room temperature with 32 scan repetitions, a resolution of 8 cm^{-1}, a gain of 4×, and a spectral range of 4000−10,000 cm^{-1}. The background signal was subtracted by using air as a reference, and each sample was acquired three times to obtain the average NIRS spectrum.

2.3.3.4. Confocal Laser Scanning Microscopy. Confocal microscopy was employed to demonstrate the adsorption of solid particles at the oil−water interface.[27] 1 mL of Pickering emulsion was mingled with 100 μL of mixed fluorescent dyes (1 mg/mL Nile red in isopropanol solution and 1 mg/mL Nile blue aqueous solution) vortexed for 5 min to ensure thorough mixing. Nile red was utilized for staining the oil phase (marked in green) with Nile blue for the modified amber particles (marked in red). After being dyed, the emulsions were placed on a microscope slide and observed under the microscope to collect the CLSM images using the multiphoton laser scanning confocal microscope SP8 DIVE (Leica Microsystems, Germany), with the fluorescent dyes being excited by differing wavelengths. Specifically, Nile is red at 488 nm and Nile blue at 633 nm.

2.4. Thermal Stability Studies of AT-EO in Pickering Emulsion. *2.4.1. Overall Performance of AT-EO in Each Group. 2.4.1.1. Retention Rate.* The retention rate of volatile oil can reflect the extent to which volatile components are preserved in the sample during the heating process. In accordance with the method described by Peng et al.,[21] a certain amount of Pickering emulsion (AT-EO with a volume fraction of 65%, 7.5 μg/mL modified amber, prepared using an IKA T18 digital high-speed disperser), a physical mixture (65% AT-EO, 7.5 μg/mL modified amber, slight stirring), and an equal amount of AT-EO were placed in 100 mL evaporating dishes separately. Then, these dishes were placed into a DHG-9140A electric hot air-drying oven (Shanghai Yiheng Scientific Instrument Co., Ltd.) with a set temperature of 40 °C for 1, 3, and 8 h, respectively. Removed and recorded the volume of AT-EO (O group). Then, the physical mixture (M group) and Pickering emulsion (P group) were distilled by a water steam distillation method for 8 h to separate AT-EO and its volume. The retention rate was calculated as follow

$$\text{retention rate}/\% = \frac{V_t}{V_0} \times 100\% \quad (3)$$

where V_t is the volume of AT-EO in each group at time t during the heat treatment process; V_0 is the initial volume of AT-EO added in each group.

2.4.1.2. Peroxide Value. The peroxide value (PV) in the samples is measured using the titration method.[23,35] The heat treatment of Pickering emulsion, physical mixture, and AT-EO was performed according to the ″2.4.1.1 Retention rate” section. The treated AT-EO was stored in the refrigerator at 4 °C. Afterward, Pickering emulsion and physical mixture were subjected to high-speed centrifugation (11,000 rpm, 30 min) to separate AT-EO, which was also stored in the refrigerator at 4 °C. 500 μL of volatile oil from each group was added to 50 mL conical flasks with stoppers, respectively. Then, 10 mL of chloroform and glacial acetic acid mixed solution (4:6) and 1 mL of saturated potassium iodide solution were accurately appended; the bottle was sealed, shook for 0.5 min, and left in a dark environment for 3 min. It was removed, along with 30 mL of water and 1 mL of 1% starch indicator. Finally, the solution was titrated with a 0.1 mol/L sodium thiosulfate standard solution until the blue color of the solution disappeared. Recorded the volume of sodium thiosulfate standard solution consumed and calculated the PV according to eq 4. Parallel to this, a blank test was established using an equivalent volume of chloroform and glacial acetic acid mixed solution, saturated potassium iodide solution, 1% starch indicator, and water, as mentioned above.

$$X = \frac{(V - V_0) \times c \times 0.1269}{m} \times 100 \quad (4)$$

where X is PV, expressed in g/100 g; V is the volume of sodium thiosulfate standard solution consumed by the sample, expressed in mL; V_0 is the volume of sodium thiosulfate standard solution consumed in the blank test, expressed in mL; c is the concentration of sodium thiosulfate standard solution, expressed in mol/L; 0.126 9 represents the mass of iodine equivalent to 1.00 mL of sodium thiosulfate standard titration solution [$c(Na_2S_2O_3)$ = 1.000 mol/L]; m is the sample mass, expressed in g; 100 is conversion factors.

2.4.1.3. Malondialdehyde. The malondialdehyde (MDA) content in the samples is determined using the spectrophotometric method.[36,37] An appropriate amount of 1,1,3,3 tetraethoxypropane was accurately weighed and diluted with water to 500 mL to prepare the MDA standard stock solution. 0, 1, 3, 5, 10, 20, 30, and 40 μL of MDA standard stock solution were pipetted directly to 10 mL volumetric flasks, separately, and diluted with water to tick mark. We finally obtained the standard curve solutions of the MDA with concentrations 0, 0.01, 0.03, 0.05, 0.1, 0.2, 0.3, and 0.4 μg/mL. Next, 5.00 mL of the above standard curve solutions were transferred into 50 mL conical flasks with stoppers, respectively. Then, 5 mL of 0.02 mol/L TBA solution was added, mixed thoroughly, and heated in a thermostat water bath at 90 °C for 40 min. Afterward, the solutions were removed and allowed to cool in the dark for 1 h. Then, 5.00 mL of chloroform was added, and the mixture was shaken well and allowed to stand for 1 h. Similarly, a blank test was established using equal volume solutions, as mentioned above. Finally, the supernatant was taken, and its absorbance was measured at 532 nm. The standard curve of MDA was plotted with the concentration of the series standard solutions as the horizontal coordinate (X) and the absorbance as the vertical coordinate (Y).

https://doi.org/10.1021/acsomega.3c08110
ACS Omega 2024, 9, 20773−20790

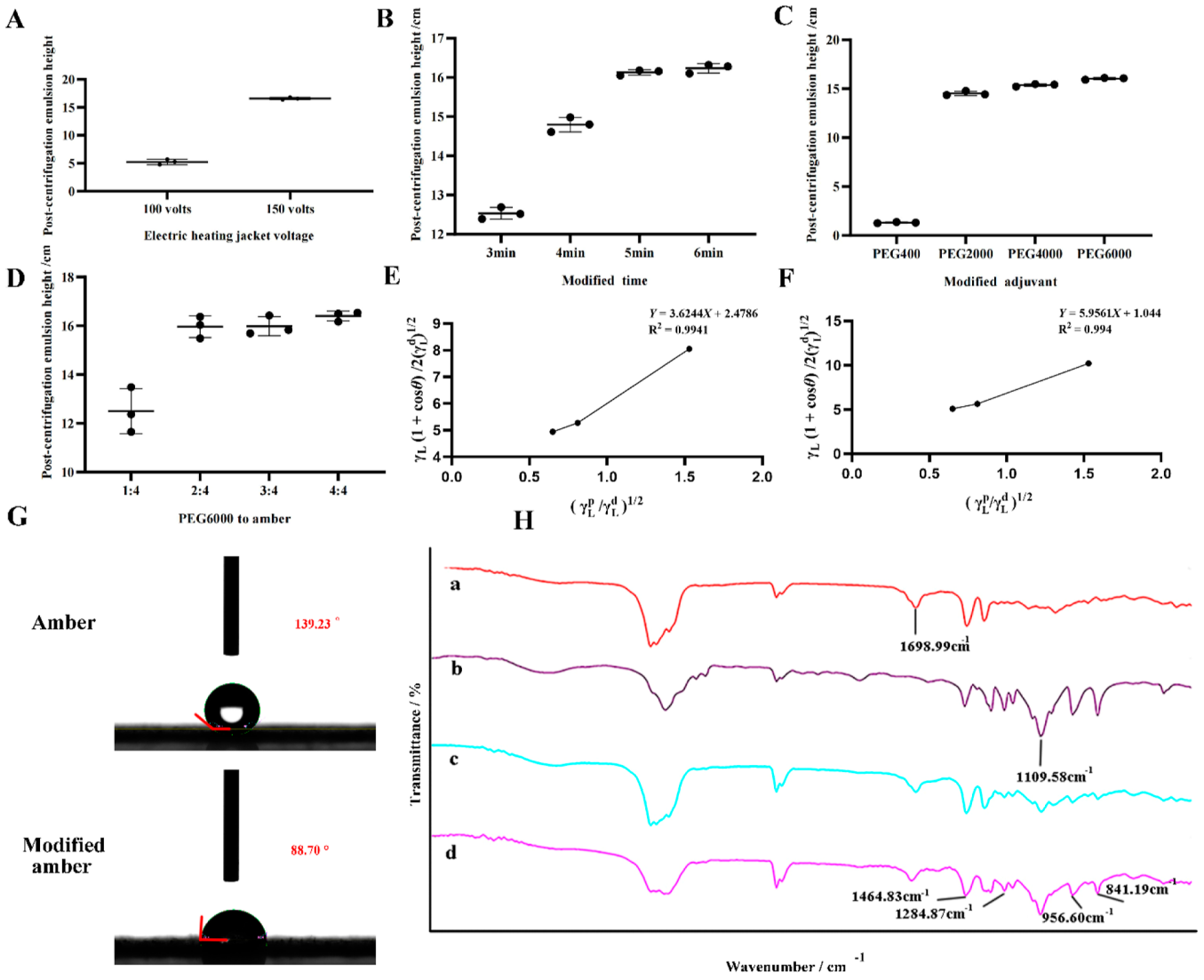

Figure 1. Single-factor investigation and characterization of modified amber particles. Results of electric heating jacket voltage (A), modification time (B), modification adjuvant (C), and the ratio of PEG6000 to amber (D). Linear curve between contact angles with the surface free energy and its components of amber (E) and modified amber particles (F). (G) Wettability of amber and modified amber particles. (H) FT-IR of amber (a), PEG6000 (b), physical mixture of amber and PEG6000 (c), and modified amber particles (d).

500 μL of volatile oil was taken from each of the three groups under the "Peroxide Value" section into a 10 mL volumetric flask individually. Then, it was diluted with the mixed solution of trichloroacetic acid to tick mark, ultrasonicated at 40 °C for 30 min, and filtered; 5.00 mL of the filtrates was collected into 50 mL conical flasks with a stopper, and 5.00 mL of TBA solution was added. It was then heated in a thermostat water bath at 90 °C for 40 min, removed, and cooled for 1 h in dark conditions. Appended 5.00 mL of chloroform was added, shaken vigorously, and allowed to settle for 1 h. Parallel to this, a blank test was established using equal volume solutions, as mentioned above. Finally, we measured the absorbance of the supernatant at 532 nm and calculated the MDA content in samples according to the standard curve of MDA.

2.4.2. Component Changes of AT-EO in Each Group. 2.4.2.1. Determination of the Volatile Components by GC–MS. Chromatographic conditions: The analysis was conducted using an HP-5MS quartz capillary column (30 m × 0.25 mm, 0.25 μm). The carrier gas was helium gas (purity 99.999%) with a flow rate of 1 mL/min. The split ratio was set at 10:1, the injection volume was 1 μL, and the injection port temperature was 230 °C. The temperature program was as follows: maintained at 50 °C for 2 min, then increased at 5 °C/min to 110 °C and held for 2 min, then ramped at 2 °C/min to 120 °C and kept for 5 min, further ascended at 0.5 °C/min to 125 °C and stayed for 10 min, then increased at 4 °C/min to 200 °C and held for 2 min, and finally rose at 10 °C/min to 250 °C and maintained for 2 min. Mass spectrometric conditions: Ionization mode EI, ion mode ESI, electron energy set at 70 eV, quadrupole temperature at 150 °C, and ion source temperature at 230 °C. The scan range was m/z 35 to 500, and the solvent delay set was 3 min.

Preparation of the sample solution: 100 μL of the volatile oil from each group under the "Peroxide Value" section was transferred to 10 mL brown volumetric flasks, respectively. Next, 100 μL of the internal standard solution (n-Docosane, 10 mg/mL) was added, and then diluted to 10 mL. Finally, the appropriate amount of anhydrous sodium sulfate was joined for dehydration, shook well, and filtered through a 0.22 μm

https://doi.org/10.1021/acsomega.3c08110
ACS Omega 2024, 9, 20773−20790

Table 2. Contact Angles of Amber and Modified Amber for Water (θ_W), Methanol (θ_M), and Ethylene Glycol (θ_E) and Its Surface Free Energy Components ($\bar{x} \pm$ SD, $n = 3$)

samples	contact angle			surface free energy		
	θ_W	θ_M	θ_E	γ_S (mJ/m^2)	γ_S^d (mJ/m^2)	γ_S^p (mJ/m^2)
amber	88.15 ± 1.22	42.18 ± 1.09	79.52 ± 1.11	19.28	6.14	13.14
modified amber	72.02 ± 1.55	37.40 ± 0.44	74.68 ± 0.8	36.57	1.09	35.48

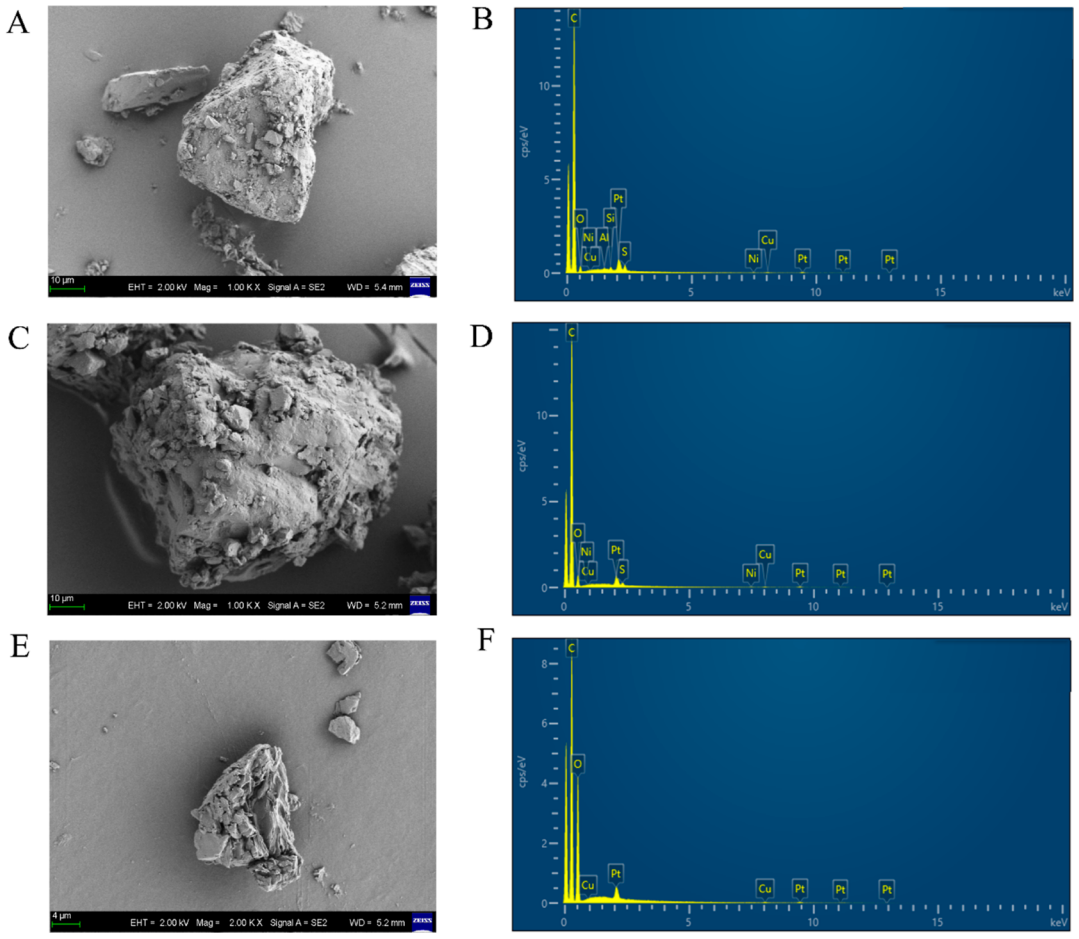

Figure 2. Surface morphology and elemental analysis of amber (A,B), modified amber (C,D), and PEG6000 (E,F).

microporous membrane into the sample vial. Analysis was performed using the aforementioned GC−MS conditions.

2.4.2.2. Screening and Analysis of Component Changes in Each Group. The GC−MS data were analyzed using Data Analysis software and compared with the W11N17main.L database for compound identification.The peak area and CAS of volatile component in each group were selected according to the matching degree ≥ 60, and the relative content of volatile component was calculated by the internal standard peak area using RStudio software with dplyr packages.[38] Differential components between AT-EO which subjected to heat treatment for 1, 3, and 8 h and untreated AT-EO were selected by the volcano plot with the criteria of Log2FC ≥ 1.5 and $P < 0.05$ using limma packages.[39] Then, a line plot was drawn to analyze the changes in relative content of differential components with ggplot2 packages.[40] The selection of qualitative components (disappearance and new formation of components) was performed for analyzing changes in composition using the OmicShare tools, a free online platform for data analysis (https://www.omicshare.com/tools).

2.5. Statistical Analysis. All experiments were conducted in triplicate, and the data were expressed as mean ± SD. Statistical analysis of significant differences was executed using one-way ANOVA tests in SPSS 26 software, with multiple comparisons performed by LSD (Homogeneity of variance) and Tambane's T2 (Unequal Variances). Statistical significance was set as follows: $*P < 0.05$, $**P < 0.01$, and $***P < 0.001$.

3. RESULTS AND DISCUSSION

3.1. Single-Factor Investigation of Modified Amber. *3.1.1. Electric Heating Jacket Voltage.* The centrifugation results of an emulsion could provide a preliminary assessment of its stability.[41] Therefore, the height of the emulsion layer after centrifugation was used as an indicator to clarify the effect of temperature on the modification of amber. As depicted in Figure 1A, at a setting of 150 V for the electric heating jacket (which equates to 230 °C), the postcentrifugation emulsion height was substantially higher than that observed at 100 V. This result indicates that the emulsification ability of the amber

https://doi.org/10.1021/acsomega.3c08110
ACS Omega 2024, 9, 20773−20790

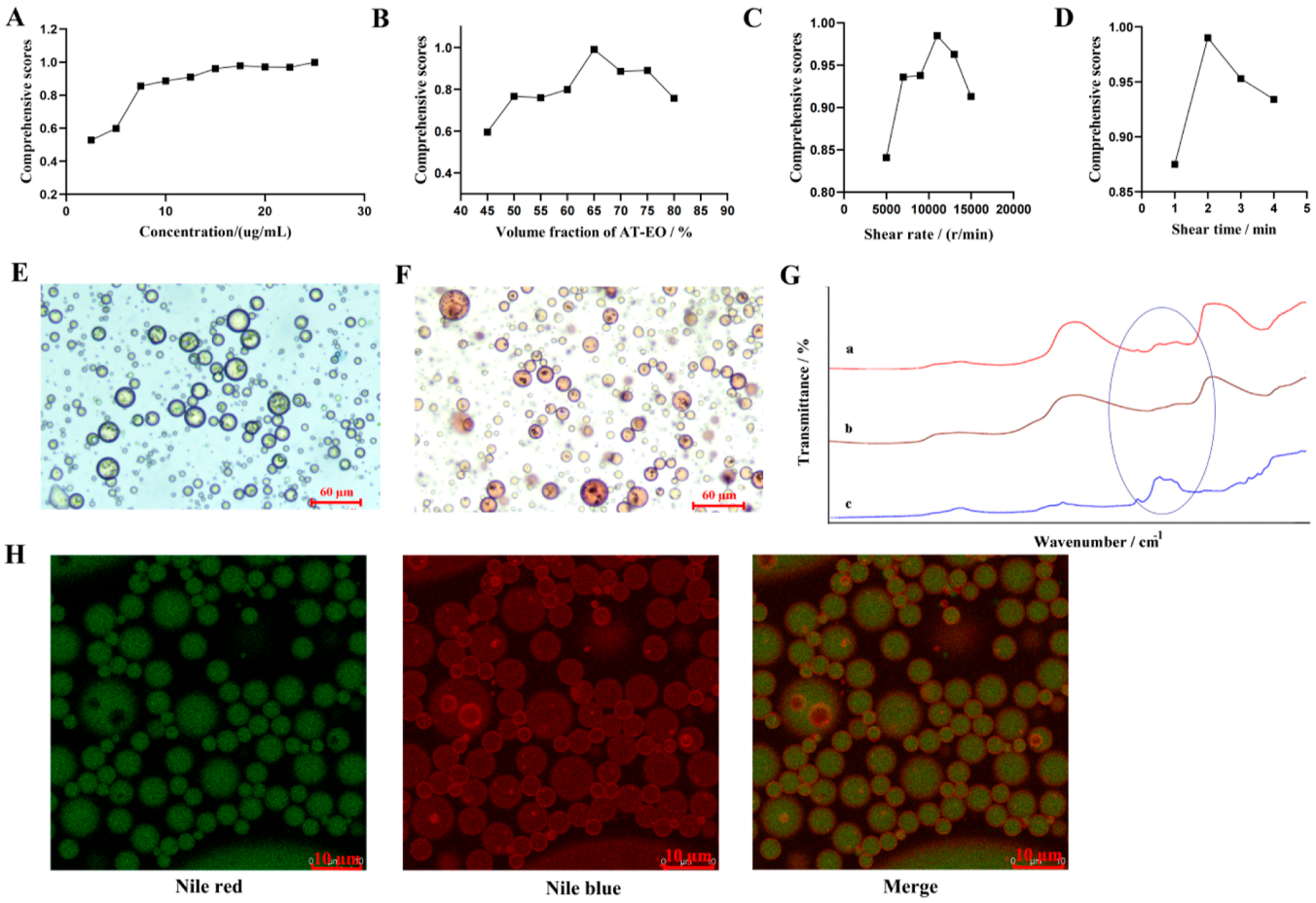

Figure 3. Single-factor investigation and characterization of Pickering emulsion. Comprehensive score results of the added amount of modified amber particles (A), volume fraction of AT-EO (B), shear rate (C), and shear time (D). Images of Pickering emulsion stained with methylene blue (E) and Sudan III (F). (G) Near-infrared spectra of Pickering emulsion (a), suspension of modified amber particles (b), and AT-EO (c). (H) Confocal microscopic images of Pickering emulsion.

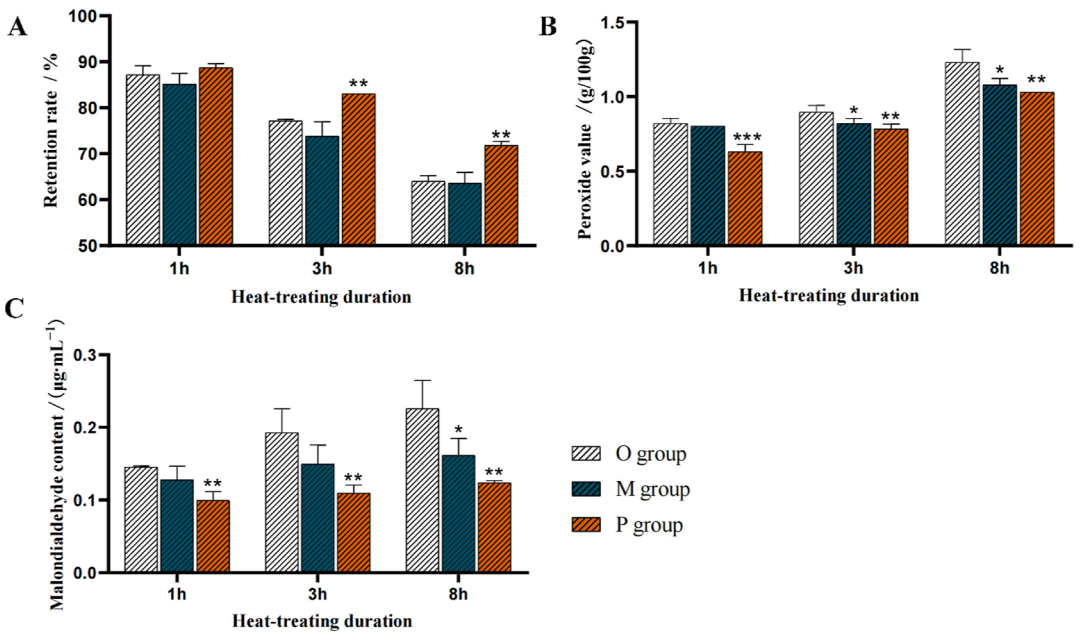

Figure 4. Retention rate (A), PV (B), and MDA content (C) of AT-EO in Pickering emulsion, physical mixture, and AT-EO group under heat treatment for 1, 3, and 8 h. Data are mean ± SD, $n = 3$; *$P < 0.05$, **$P < 0.01$, and ***$P < 0.001$ vs the AT-EO group.

https://doi.org/10.1021/acsomega.3c08110
ACS Omega 2024, 9, 20773−20790

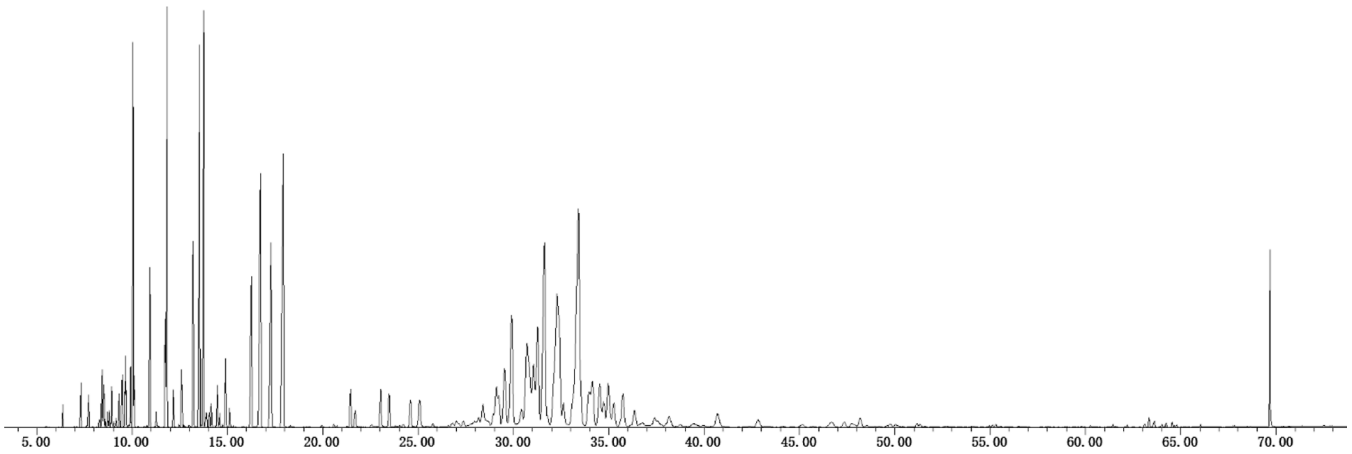

Figure 5. Total ion flowchart of AT-EO.

prepared under 150 V was superior, resulting in a more stable emulsion.

3.1.2. Modification Time. As was shown in Figure 1B, it was apparent that the postcentrifugation emulsion height augmented substantially with the extended modification time. However, the difference in the height of the emulsion layer between modification times of 5 and 6 min was not significant. To avoid unnecessary losses, we ultimately determined the modification time to be 5 min.

3.1.3. Modification Adjuvant. Polyethylene glycol (PEG) exhibits excellent water solubility, and PEG4000 and PEG6000 are especially favored for their low toxicity and stable chemical properties.[41] These attributes make PEG an ideal choice as a modifier adjuvant for increasing the hydrophilicity of amber. Figure 1C demonstrates that the emulsion layer reached its maximum height when PEG6000 was used as the modifying adjuvant. Therefore, PEG6000 was selected as the preferred modifier.

3.1.4. Ratio of PEG6000 to Amber. Further research was conducted to assess the effect of the ratio between PEG6000 and amber on the modification effectiveness. As depicted in Figure 1D, Pickering emulsions stabilized by modified amber were prepared at ratios of 2:4, 3:4, and 4:4, showing higher emulsion layer heights compared to those at a 1:4 ratio. In order to minimize the use of adjuvant, the optimal ratio of PEG6000 to amber was established to be 1:2.

The final modification method for amber was as follows: PEG6000 and amber were accurately weighed in a ratio of 1:2, the PEG6000 was placed in an evaporating dish, and heated using an electric heating sleeve (150 V, preheated for 10 min) until melting. Next, the amber powder was added, and the mixture was vigorously stirred with a glass rod for 5 min to ensure a full mix of PEG6000 and amber. After drying for 24 h, the mixture was ground, and the modified amber was acquired by passing it through a sieve (no. 5).

3.2. Characterization of Modified Amber. *3.2.1. Surface Free Energy.* Relevant literature indicates that surface free energy, including polar and nonpolar components, is the fundamental thermodynamic property of a solid surface, closely related to various surface properties such as wettability, adhesion, and adsorption.[29] Owens−Wendt−Rabel−Kaelble model was utilized to elucidate the surface free energy of both modified amber and amber. Linear relationships between the contact angles and the surface free energy components of amber (Figure 1E) and modified amber (Figure 1F) was depicted, and its corresponding values are presented in Table 2. Notably, the surface free energy and polar component of modified amber were higher in comparison to the amber, concurrent with an increase in wettability. These findings indicate that samples with reduced contact angles are correlate with elevated surface energy and its polar component, which aligns with relevant researches.[42,43] Meanwhile, these results affirm the effective modification of amber, which might be the key to the successful preparation of oil-in-water Pickering emulsions with modified amber particles.

3.2.2. Wettability. The images of contact angles for both amber and modified amber are shown in Figure 1G. θ_{aw} of amber was 139.23 ± 2.41°, indicating that amber was highly hydrophobic. After surface modification with PEG6000, the θ_{aw} of modified amber decreased to 88.70 ± 1.18°, showing a great improvement in the hydrophilicity of modified amber. This finding demonstrated that PEG6000 has successfully modified the surface properties of amber.

3.2.3. Fourier Transform Infrared Spectroscopy. The infrared spectra of the modified amber particles and PEG6000 were very similar (Figure 1H). The spectrum of modified amber showcased a characteristic peak of amber around 1700 cm^{-1}, which is absent in the spectrum of PEG6000. Simultaneously, the peaks observed at 1464.83, 1284.87, 1109.58, 956.60, and 841.19 cm^{-1} in the spectrum of modified amber corresponded to the characteristic absorption peaks of PEG6000. The spectrum of the physical mixture displayed a simple superimposition of the absorption peaks of amber and PEG6000. The infrared spectra provided evidence that the surface composition of the modified amber bore a significant resemblance to PEG6000, indicating that PEG6000 successfully modified the amber by the melting method.

3.2.4. Scanning Electron Microscope and Energy-Dispersive X-ray Spectroscopy Analysis. Figure 2 presents the high-resolution images and elemental analysis results of amber, PEG6000, and modified amber particles. The amber particles appeared as elongated blocks, with a surface covered by unevenly distributed particles of various sizes. The cross-section of PEG6000 exhibited a layered structure. As shown in Figure 2C, the modified amber particles exhibited the phenomenon of the aggregation formation of multiple particles. These findings indicated that PEG6000 interacted with amber during the melting process, causing alterations in the surface morphology of the modified amber particles.

https://doi.org/10.1021/acsomega.3c08110
ACS Omega 2024, 9, 20773−20790

Table 3. Relative Content of Volatile Components in Pickering Emulsion, Physical Mixture, and AT-EO Groups After Heat Treatment for 1, 3, and 8 h ($\bar{x} \pm$ SD, $n = 3$)

CAS	compound name	untreated AT-EO	1h-M	1h-O	1h-P	3h-M	3h-O	3h-P	8h-M	8h-O	8h-P
007785-26-4	(1*S*)-(−)-*α*-pinene	2.1391 ± 0.1300	0.1665 ± 0.2884	0.3239 ± 0.2863	1.8980 ± 0.0201	0.0000 ± 0.0000	0.0000 ± 0.0000	1.6459 ± 0.0461	0.0000 ± 0.0000	0.0000 ± 0.0000	1.2326 ± 0.0823
005794-04-7	bicyclo[2.2.1]heptane	1.8107 ± 0.1041	0.1749 ± 0.3030	0.1902 ± 0.3295	1.6115 ± 0.0202	0.0000 ± 0.0000	0.0000 ± 0.0000	1.3767 ± 0.0345	0.0000 ± 0.0000	0.0000 ± 0.0000	1.0279 ± 0.0411
003387-41-5	sabinene	3.0565 ± 0.1746	1.0272 ± 0.1147	1.1059 ± 0.1153	2.6733 ± 0.0766	0.0000 ± 0.0000	0.0000 ± 0.0000	2.3201 ± 0.0324	0.0000 ± 0.0000	0.0000 ± 0.0000	1.7282 ± 0.1277
000127-91-3	*β*-pinene	2.3184 ± 0.1389	0.7477 ± 0.0821	0.7971 ± 0.0862	1.9924 ± 0.0831	0.0000 ± 0.0000	0.0000 ± 0.0000	1.7334 ± 0.0357	0.0000 ± 0.0000	0.0000 ± 0.0000	1.3312 ± 0.1156
000500-00-5	*p*-menth-3-ene	0.8100 ± 0.0440	0.0000 ± 0.0000	0.0000 ± 0.0000	0.7119 ± 0.0118	0.0000 ± 0.0000	0.0000 ± 0.0000	0.6255 ± 0.0129	0.0000 ± 0.0000	0.0000 ± 0.0000	0.4887 ± 0.0345
000110-93-0	6-methyl-5-hepten-2-one	0.7915 ± 0.0497	0.4817 ± 0.0253	0.4971 ± 0.0168	0.6689 ± 0.0260	0.0000 ± 0.0000	0.0000 ± 0.0000	0.0000 ± 0.0000	0.0000 ± 0.0000	0.0000 ± 0.0000	0.0000 ± 0.0000
000123-35-3	myrcene	1.9794 ± 0.1166	0.9204 ± 0.0703	0.9679 ± 0.0626	1.7639 ± 0.0126	0.0000 ± 0.0000	0.0000 ± 0.0000	1.5295 ± 0.0264	0.0000 ± 0.0000	0.0000 ± 0.0000	1.1293 ± 0.0754
000124-18-5	decane	0.3592 ± 0.3118	0.0000 ± 0.0000	0.0000 ± 0.0000	0.0000 ± 0.0000	0.0000 ± 0.0000	0.0000 ± 0.0000	0.0000 ± 0.0000	0.0000 ± 0.0000	0.0000 ± 0.0000	0.2803 ± 0.2428
000099-83-2	*α*-phellandrene	1.9303 ± 0.1020	0.9019 ± 0.0667	0.9466 ± 0.0592	1.6539 ± 0.0275	0.0000 ± 0.0000	0.0000 ± 0.0000	1.4259 ± 0.0303	0.0000 ± 0.0000	0.0000 ± 0.0000	1.0295 ± 0.0632
007785-70-8	(1*R*)-(+)-*α*-pinene	2.6562 ± 0.1384	1.1978 ± 0.0950	1.2542 ± 0.0855	2.4110 ± 0.0145	0.0000 ± 0.0000	0.0000 ± 0.0000	2.1019 ± 0.0417	0.0000 ± 0.0000	0.0000 ± 0.0000	1.5720 ± 0.0980
000470-67-7	1,4-cineole	2.2430 ± 0.1165	1.3107 ± 0.0778	1.3503 ± 0.0565	1.2863 ± 1.1140	0.5145 ± 0.0432	0.4257 ± 0.2497	1.4550 ± 0.0227	0.0000 ± 0.0000	0.0000 ± 0.0000	0.4251 ± 0.3682
029050-33-7	(+)-4-carene	3.8030 ± 0.2241	1.9297 ± 0.1349	2.0005 ± 0.0931	3.1635 ± 0.1055	0.5439 ± 0.0555	0.4245 ± 0.3678	2.7070 ± 0.0612	0.0000 ± 0.0000	0.0000 ± 0.0000	1.8769 ± 0.1062
000099-87-6	*p*-cymene	3.4023 ± 0.2029	2.1622 ± 0.1077	2.2329 ± 0.1578	4.3641 ± 0.2267	1.0110 ± 0.0898	1.0407 ± 0.0697	4.0863 ± 0.0850	0.0000 ± 0.0000	0.0000 ± 0.0000	3.2000 ± 0.1994
000464-17-5	2-bornene	21.9550 ± 1.5394	14.1063 ± 0.7790	14.5061 ± 0.5670	22.2027 ± 0.1006	5.3401 ± 0.4447	5.6500 ± 0.5850	19.7269 ± 0.3242	0.1573 ± 0.2725	0.3464 ± 0.3208	14.8618 ± 0.8575
000470-82-6	cineole	2.2211 ± 0.1297	1.4622 ± 0.0748	1.4954 ± 0.0457	2.0164 ± 0.0423	0.6743 ± 0.0457	0.7091 ± 0.0516	1.5219 ± 0.0196	0.0000 ± 0.0000	0.0000 ± 0.0000	0.7087 ± 0.0044
000508-32-7	cyclene	8.2972 ± 0.4554	5.5224 ± 0.2600	5.6377 ± 0.0931	7.1668 ± 0.1599	2.6305 ± 0.1403	2.7963 ± 0.1799	6.1819 ± 0.1225	0.1378 ± 0.2387	0.3375 ± 0.3043	4.2918 ± 0.2491
000586-67-4	1-isopropenyl-4-methylcyclohexene	0.8846 ± 0.0515	0.6111 ± 0.0108	0.6404 ± 0.0104	0.8305 ± 0.0031	0.0000 ± 0.0000	0.0000 ± 0.0000	0.7247 ± 0.0069	0.0000 ± 0.0000	0.0000 ± 0.0000	0.5179 ± 0.0286
000099-86-5	*α*-terpinene	5.8785 ± 0.3504	4.2020 ± 0.1624	4.2718 ± 0.0417	5.1973 ± 0.1224	2.3290 ± 0.0984	2.4682 ± 0.1102	4.4919 ± 0.0879	0.1746 ± 0.3023	0.4220 ± 0.3769	3.1213 ± 0.1747
000586-62-9	terpinolene	26.8584 ± 1.4813	20.4528 ± 0.7378	20.6433 ± 0.1618	25.7462 ± 0.3158	12.3380 ± 0.3885	13.0004 ± 0.4424	22.7079 ± 0.3071	2.4568 ± 0.5432	3.1871 ± 1.0125	16.2282 ± 0.8455
000078-70-6	linalool	2.0204 ± 0.1262	1.8868 ± 0.0277	1.8787 ± 0.0475	2.0669 ± 0.0350	1.7779 ± 0.0227	1.8675 ± 0.0481	1.9047 ± 0.0241	1.2986 ± 0.0694	1.4083 ± 0.1222	1.4213 ± 0.0605
001632-73-1	(1*R*)-(+)-fenchyl alcohol	3.1612 ± 0.1838	2.9797 ± 0.0595	2.9743 ± 0.0610	3.2645 ± 0.0608	2.8372 ± 0.0357	2.9875 ± 0.0928	3.0237 ± 0.0178	2.1087 ± 0.1144	2.2800 ± 0.1972	2.2803 ± 0.0773
000586-82-3	3-cyclohexen-1-ol, 1-methyl-4-(1-methylethyl)-	11.1461 ± 0.6424	10.6903 ± 0.2088	10.6912 ± 0.2356	11.8907 ± 0.2053	10.4205 ± 0.1506	10.9890 ± 0.3877	11.2228 ± 0.0550	8.5611 ± 0.3368	9.1337 ± 0.5868	8.7477 ± 0.2785
000138-87-4	1-methyl-4-prop-1-en-2-ylcyclohexan-1-ol	29.9988 ± 1.6040	29.3350 ± 0.5590	29.2630 ± 0.6344	32.8727 ± 0.5221	29.1973 ± 0.6383	30.7708 ± 1.1506	31.6657 ± 0.0959	24.5051 ± 1.9345	26.6351 ± 2.5549	25.5602 ± 0.9269
000106-23-0	citronellal	31.0869 ± 1.6945	29.4868 ± 0.6037	29.4017 ± 0.5968	32.5313 ± 0.3382	27.2886 ± 0.5021	28.7184 ± 0.8828	30.1045 ± 0.1304	19.7819 ± 1.8006	21.3464 ± 2.8618	22.9842 ± 0.9324

https://doi.org/10.1021/acsomega.3c08110
ACS Omega 2024, 9, 20773−20790

Table 3. continued

CAS	compound name	untreated AT-EO	1h-M	1h-O	1h-P	3h-M	3h-O	3h-P	8h-M	8h-O	8h-P
000124-76-5	DL-isoborneol	1.2649 ± 0.3934	1.1671 ± 0.3171	1.0244 ± 0.0593	1.0968 ± 0.0150	0.9758 ± 0.0132	1.2084 ± 0.3344	1.0433 ± 0.0045	1.1256 ± 0.0453	1.2165 ± 0.0889	1.1093 ± 0.2522
000464-45-9	L-(−)-borneol	1.4294 ± 0.0761	1.3728 ± 0.0327	1.3849 ± 0.0500	1.5045 ± 0.0277	1.3843 ± 0.0311	1.4739 ± 0.0778	1.4591 ± 0.0043	1.2623 ± 0.0314	1.3448 ± 0.0583	1.2307 ± 0.0504
000562-74-3	terpinen-4-ol	2.3404 ± 0.1415	2.2268 ± 0.0483	2.2267 ± 0.0450	2.4343 ± 0.0310	2.1784 ± 0.0448	2.3033 ± 0.0769	2.3178 ± 0.0089	1.7971 ± 0.0805	1.9120 ± 0.1184	1.8336 ± 0.0531
055722-59-3	isocitral	0.8082 ± 0.0540	0.7858 ± 0.0233	0.7794 ± 0.0294	0.7621 ± 0.0148	0.7612 ± 0.0385	0.8071 ± 0.0266	0.7252 ± 0.0084	0.6934 ± 0.0290	0.7096 ± 0.0194	0.5969 ± 0.0165
000098-55-5	α-terpineol	4.1003 ± 0.2323	4.0465 ± 0.0596	4.0445 ± 0.0988	4.4800 ± 0.0595	4.1972 ± 0.1128	4.4503 ± 0.2070	4.4342 ± 0.0111	4.0659 ± 0.0685	4.2743 ± 0.1317	3.8263 ± 0.1419
000586-81-2	γ-terpineol	1.1865 ± 0.0851	1.1345 ± 0.0116	1.1395 ± 0.0315	1.2713 ± 0.0189	1.1637 ± 0.0324	1.2543 ± 0.0804	1.2609 ± 0.0036	1.1217 ± 0.0179	1.1835 ± 0.0388	1.0464 ± 0.0353
001117-61-9	(*R*)-citronellol	13.7612 ± 0.7702	14.0053 ± 0.1676	13.9054 ± 0.4124	14.9131 ± 0.1866	15.0604 ± 0.4921	15.8176 ± 0.7552	15.1454 ± 0.0650	16.0902 ± 0.1155	16.6222 ± 0.3359	14.2081 ± 0.5289
000106-26-3	*cis*-citral	27.3900 ± 1.7686	25.6221 ± 0.3904	25.4773 ± 0.6684	27.9673 ± 0.2464	25.8358 ± 0.7187	27.2745 ± 1.0380	27.2648 ± 0.1540	24.1835 ± 0.4973	25.3996 ± 0.8911	22.6697 ± 0.7841
000106-24-1	geraniol	20.5694 ± 1.1285	21.1080 ± 0.2590	20.9344 ± 0.5935	22.6188 ± 0.2674	22.7268 ± 0.7707	23.9106 ± 1.1614	23.0082 ± 0.0737	24.5790 ± 0.2073	25.4322 ± 0.5323	21.7478 ± 0.8368
000141-27-5	*trans*-3,7-dimethyl-octa-2,6-dien-1-al	32.2474 ± 1.7304	32.4242 ± 0.4878	32.1753 ± 0.8099	35.2336 ± 0.3776	33.5988 ± 0.9880	35.4373 ± 1.5396	36.8687 ± 3.1931	33.5100 ± 0.4748	34.9078 ± 0.8679	30.7161 ± 1.0337
002792-39-4	(6*E*)-2,6-dimethylocta-2,6-diene	3.1946 ± 0.1855	3.2546 ± 0.0414	3.2308 ± 0.0843	3.5133 ± 0.0455	3.5288 ± 0.1022	3.6991 ± 0.2016	3.6258 ± 0.0043	3.7909 ± 0.0367	3.9000 ± 0.0600	3.4003 ± 0.0822
000097-53-0	eugenol	1.5993 ± 0.0842	1.6344 ± 0.0244	1.6168 ± 0.0671	1.7133 ± 0.0334	1.8806 ± 0.0202	1.9285 ± 0.1308	1.7217 ± 0.0367	2.2072 ± 0.0279	2.1827 ± 0.0160	1.7783 ± 0.0533
000141-12-8	neryl acetate	3.7923 ± 0.2312	3.8481 ± 0.0534	3.7631 ± 0.1211	4.0564 ± 0.0544	4.1706 ± 0.1595	4.4114 ± 0.2266	4.2002 ± 0.0373	4.6088 ± 0.0211	4.7069 ± 0.0753	4.0137 ± 0.1144
000515-13-9	β-elemen	3.5466 ± 0.2149	3.5567 ± 0.0354	3.5285 ± 0.0869	3.9560 ± 0.0398	3.8507 ± 0.1241	4.0345 ± 0.2050	4.0310 ± 0.0178	4.1037 ± 0.0348	4.2202 ± 0.0734	3.6109 ± 0.0958
000469-61-4	α-cedrene	3.1774 ± 0.1810	3.2026 ± 0.0378	3.1921 ± 0.0765	3.5590 ± 0.0414	3.4082 ± 0.1134	3.5890 ± 0.1737	3.6040 ± 0.0129	3.5528 ± 0.0391	3.7419 ± 0.1373	3.1467 ± 0.0838
000546-28-1	(+)-β-cedrene	4.4961 ± 0.2528	4.5516 ± 0.0538	4.5196 ± 0.1137	5.0245 ± 0.0472	4.8324 ± 0.1496	5.1106 ± 0.2767	5.0936 ± 0.0348	5.0880 ± 0.0194	5.2474 ± 0.1129	4.4839 ± 0.0865
094535-52-1	(1*R*,3a*S*,4a*S*,8a*S*)-1,4,4,6-tetramethyl-1,2,3,3a,4,4a,7,8-octahydrocyclopenta[1,4]cyclobuta[1,2]benzene	4.0369 ± 0.9497	3.5139 ± 1.1326	3.5524 ± 1.3066	3.8548 ± 0.9402	3.5795 ± 1.9491	5.0752 ± 1.8124	5.1120 ± 1.5161	5.2038 ± 2.7222	5.9817 ± 2.0376	3.9787 ± 1.7524
103827-22-1	4a,8-dimethyl-2-(prop-1-en-2-yl)-1,2,3,4,4a,5,6,7-octahydronaphthalene	8.0607 ± 0.1699	7.7881 ± 0.6151	7.8096 ± 0.8013	8.7993 ± 0.5366	9.1704 ± 0.6915	9.4025 ± 1.1989	9.6557 ± 0.7774	10.8832 ± 0.3634	10.6456 ± 0.5740	8.2161 ± 0.7983
030021-74-0	γ-muurolene	3.9750 ± 0.0607	4.0328 ± 0.2885	3.9718 ± 0.3964	4.3296 ± 0.4403	4.5558 ± 0.3189	4.7944 ± 0.5281	4.8539 ± 0.1661	5.3313 ± 0.1832	5.1220 ± 0.2964	4.2778 ± 0.2495
014912-44-8	tricyclo[4.4.0.0^{2,7}]dec-3-ene, 1,3-dimethyl-8-(1-methylethyl)-, stereoisomer	10.6177 ± 0.3155	10.6984 ± 0.2873	10.6603 ± 0.6733	11.5447 ± 0.3469	11.8589 ± 0.5047	12.3796 ± 1.0853	12.2368 ± 0.4788	13.5454 ± 0.3907	13.4246 ± 0.3473	10.7034 ± 0.3914
017066-67-0	β-selinene	20.3626 ± 0.8802	21.0715 ± 0.2126	20.9257 ± 0.8636	24.0853 ± 0.6916	23.6021 ± 0.6898	24.5909 ± 1.7508	25.6765 ± 0.5034	27.4074 ± 0.6224	27.5055 ± 0.2921	23.8472 ± 0.3024
005951-61-1	β-cadinene	3.0901 ± 0.3037	3.1705 ± 0.2844	3.1636 ± 0.3889	3.4967 ± 0.2706	3.7082 ± 0.4032	3.7995 ± 0.5380	3.8625 ± 0.3417	4.6258 ± 0.3740	4.2521 ± 0.4034	3.2468 ± 0.3843
000473-13-2	α-selinene	27.2759 ± 1.3703	28.0021 ± 0.0319	27.8105 ± 0.9477	31.5566 ± 0.5143	30.7666 ± 0.9186	32.2488 ± 1.8907	33.0910 ± 0.3720	34.9455 ± 0.7724	35.2436 ± 0.4094	30.1358 ± 0.2612
029621-78-1	1-methyl-4-(1,2,2-trimethylcyclopentyl)cyclohexa-1,3-diene	12.1400 ± 0.5810	12.3243 ± 0.0624	12.2603 ± 0.4716	13.0778 ± 0.2883	13.0234 ± 0.5179	13.7490 ± 0.8640	13.5000 ± 0.2023	14.2159 ± 0.4239	14.5010 ± 0.0552	11.4155 ± 0.0786

https://doi.org/10.1021/acsomega.3c08110
ACS Omega 2024, 9, 20773−20790

Table 3. continued

CAS	compound name	untreated AT-EO	1h-M	1h-O	1h-P	3h-M	3h-O	3h-P	8h-M	8h-O	8h-P
010208-80-7	α-muurolene	18.5850 ± 0.9814	19.2048 ± 0.1622	19.0825 ± 0.5010	21.6056 ± 0.2577	21.1365 ± 0.7595	22.1570 ± 1.3498	22.6836 ± 0.1873	24.1496 ± 0.5993	24.4310 ± 0.3818	21.0966 ± 0.3204
016982-00-6	1-methyl-4-[(1*R*)-1,2,2-trimethylcyclopentyl]benzene	35.9387 ± 2.1549	37.2443 ± 0.6244	37.0318 ± 0.5492	43.4266 ± 0.5858	41.4625 ± 1.5153	43.3905 ± 2.4182	45.6769 ± 0.5034	47.5131 ± 1.1715	48.0702 ± 0.7471	42.1302 ± 0.6980
028400-12-6	α-alaskene	49.4840 ± 2.5711	51.1113 ± 0.5296	46.1094 ± 7.1974	57.0556 ± 0.6704	50.8579 ± 7.9914	53.8523 ± 10.3600	59.5963 ± 0.6430	57.8712 ± 10.3045	52.7853 ± 9.7815	45.2699 ± 7.4607
016204-67-4	1,1,4,5,6-pentamethyl-2,3-dihydro-1*H*-indene	3.6641 ± 0.2125	3.7865 ± 0.0538	3.7701 ± 0.0869	4.2416 ± 0.0401	4.1843 ± 0.1686	4.3654 ± 0.2216	4.4152 ± 0.0448	5.0386 ± 0.5803	4.8279 ± 0.0763	4.0617 ± 0.0748
000483-76-1	(+)-δ-cadinene	63.2065 ± 3.2674	65.3416 ± 0.7279	64.9086 ± 1.6657	74.2508 ± 0.9021	71.1198 ± 2.8358	74.5921 ± 3.9955	77.6700 ± 0.7634	81.1128 ± 1.8215	82.0361 ± 1.6611	70.6523 ± 1.3146
997220-96-6	γ-curcumene	6.8008 ± 0.2919	6.9713 ± 0.0940	4.3725 ± 3.7933	6.5887 ± 0.4895	7.1752 ± 0.3581	7.7337 ± 0.5541	6.8589 ± 0.3661	5.1231 ± 4.4488	7.4358 ± 0.8116	3.7514 ± 3.2578
053585-13-0	(4*E*)-1-methyl-4-(6-methylhept-5-en-2-ylidene)cyclohexene	9.3774 ± 0.6804	9.5652 ± 0.0917	9.7420 ± 0.1299	11.1180 ± 0.2061	10.5977 ± 0.3837	11.0195 ± 0.4741	11.5163 ± 0.3673	12.0747 ± 0.4077	12.7401 ± 0.7820	12.6368 ± 3.4464
024406-05-1	α-cadinene	8.2525 ± 0.4389	8.5315 ± 0.1010	8.4966 ± 0.2056	9.5304 ± 0.0991	9.3078 ± 0.3974	9.8388 ± 0.5772	10.0065 ± 0.1001	10.6411 ± 0.3013	10.8407 ± 0.2241	9.1916 ± 0.2142
000515-17-3	γ-selinene	4.5314 ± 0.2616	4.6723 ± 0.0203	4.6595 ± 0.1422	5.2676 ± 0.0868	5.1507 ± 0.1867	5.3891 ± 0.2754	5.5358 ± 0.0445	5.8893 ± 0.0833	5.9676 ± 0.1413	5.1523 ± 0.0793
021391-99-1	α-calacorene	8.8721 ± 0.4742	9.1656 ± 0.0787	9.1277 ± 0.2238	10.6103 ± 0.1394	10.0965 ± 0.3826	10.6208 ± 0.5821	11.1528 ± 0.1153	11.6427 ± 0.2356	11.7964 ± 0.2898	10.1880 ± 0.2127
017627-44-0	α-bisabolene	4.3185 ± 0.2173	4.4424 ± 0.0454	4.4259 ± 0.1008	4.8476 ± 0.0651	4.8639 ± 0.2141	5.1043 ± 0.2764	5.1054 ± 0.0576	5.5879 ± 0.1606	5.6570 ± 0.1382	4.8065 ± 0.0881
021657-90-9	hedycaryol	6.5893 ± 0.3520	6.8305 ± 0.0622	6.7787 ± 0.1693	7.5988 ± 0.0836	7.6211 ± 0.3174	7.9625 ± 0.4456	7.9951 ± 0.0745	8.9851 ± 0.2049	9.0342 ± 0.2533	7.7297 ± 0.2233
158930-41-7	eremophila ketone	2.9583 ± 0.1531	3.0899 ± 0.0215	3.0653 ± 0.0581	3.4839 ± 0.0341	3.4004 ± 0.1479	3.5555 ± 0.1991	3.6667 ± 0.0433	3.9166 ± 0.0614	3.9748 ± 0.0826	3.4501 ± 0.0719
020321-73-7	7-methoxy-2,2-dimethyl-3*H*-chromen-4-one	1.6519 ± 1.4316	2.5882 ± 0.0628	2.5547 ± 0.2026	2.8345 ± 0.0315	2.9599 ± 0.0796	3.0075 ± 0.3028	3.0066 ± 0.0376	3.5420 ± 0.1279	3.4297 ± 0.1835	3.0107 ± 0.0468
000077-53-2	(+)-cedrol	3.3764 ± 0.2452	3.4139 ± 0.0491	3.4469 ± 0.2494	3.7316 ± 0.1237	4.1701 ± 0.1750	4.2058 ± 0.4127	4.2751 ± 0.2150	5.1146 ± 0.1308	4.9829 ± 0.1605	4.3582 ± 0.0837
002050-24-0	1,3-diethyl-5-methylbenzene	0.5026 ± 0.4367	0.7531 ± 0.0049	0.5054 ± 0.4378	0.0000 ± 0.0000	0.8516 ± 0.0386	0.8907 ± 0.0537	0.8987 ± 0.0245	1.0735 ± 0.0230	1.0656 ± 0.0374	0.9087 ± 0.0078
007786-67-6	5-methyl-2-prop-1-en-2-yl-cyclohexan-1-ol	0.3464 ± 0.3000	0.3137 ± 0.2719	0.3194 ± 0.2771	0.0000 ± 0.0000	0.1388 ± 0.2404	0.0000 ± 0.0000	0.0000 ± 0.0000	0.0000 ± 0.0000	0.0000 ± 0.0000	0.0000 ± 0.0000
000481-34-5	(1*R*,4*S*,4a*R*,8a*R*)-4-isopropyl-1,6-dimethyl-1,2,3,4,4A,7,8,8A-octahydro-1-naphthalenol	0.0000 ± 0.0000	0.0000 ± 0.0000	0.0000 ± 0.0000	0.0000 ± 0.0000	1.8042 ± 0.1367	1.9193 ± 0.1390	0.6477 ± 1.1218	2.5961 ± 0.0634	2.5909 ± 0.0821	1.9193 ± 0.0560
913176-41-7	4,8,11,11-tetramethylbicyclo[7.2.0]undec-3-en-5-ol	0.0000 ± 0.0000	0.0000 ± 0.0000	0.0000 ± 0.0000	0.0000 ± 0.0000	1.8355 ± 1.5960	1.9872 ± 1.7722	0.0000 ± 0.0000	1.2058 ± 0.9933	2.5365 ± 1.7775	3.0002 ± 0.0655
997220-41-0	italicene	0.0000 ± 0.0000	0.0000 ± 0.0000	0.0000 ± 0.0000	0.0000 ± 0.0000	0.0000 ± 0.0000	0.6228 ± 1.0788	0.0000 ± 0.0000	1.4641 ± 1.2705	1.6915 ± 0.7737	1.0420 ± 0.6801
003856-25-5	(−)-α-copaene	0.0000 ± 0.0000	0.0000 ± 0.0000	4.6793 ± 8.1047	0.0000 ± 0.0000	4.8247 ± 8.3566	4.5158 ± 7.8216	0.0000 ± 0.0000	5.3325 ± 9.2362	11.2132 ± 9.7207	9.6687 ± 8.3734
110983-38-5	phenol, 2-(2-[1,1′-biphenyl]-4-ylethenyl)-, (*E*)-(9CI)	0.0000 ± 0.0000	0.0000 ± 0.0000	0.0000 ± 0.0000	0.0000 ± 0.0000	0.0000 ± 0.0000	0.0000 ± 0.0000	0.0000 ± 0.0000	1.0010 ± 0.0282	0.9994 ± 0.0282	0.5578 ± 0.4831
000768-91-2	1-methyladamantane	0.0000 ± 0.0000	0.0000 ± 0.0000	0.0000 ± 0.0000	0.0000 ± 0.0000	0.0000 ± 0.0000	0.0000 ± 0.0000	0.0000 ± 0.0000	0.0000 ± 0.0000	0.0000 ± 0.0000	0.3083 ± 0.2680
997332-93-7	2-pentenoic acid, 3-methyl-5-(2,6,6-trimethyl-1-cyclohexenyl)	0.0000 ± 0.0000	0.0000 ± 0.0000	0.0000 ± 0.0000	0.0000 ± 0.0000	0.0000 ± 0.0000	0.0000 ± 0.0000	0.0000 ± 0.0000	0.0000 ± 0.0000	0.0000 ± 0.0000	0.7542 ± 1.3063

https://doi.org/10.1021/acsomega.3c08110
ACS Omega 2024, 9, 20773−20790

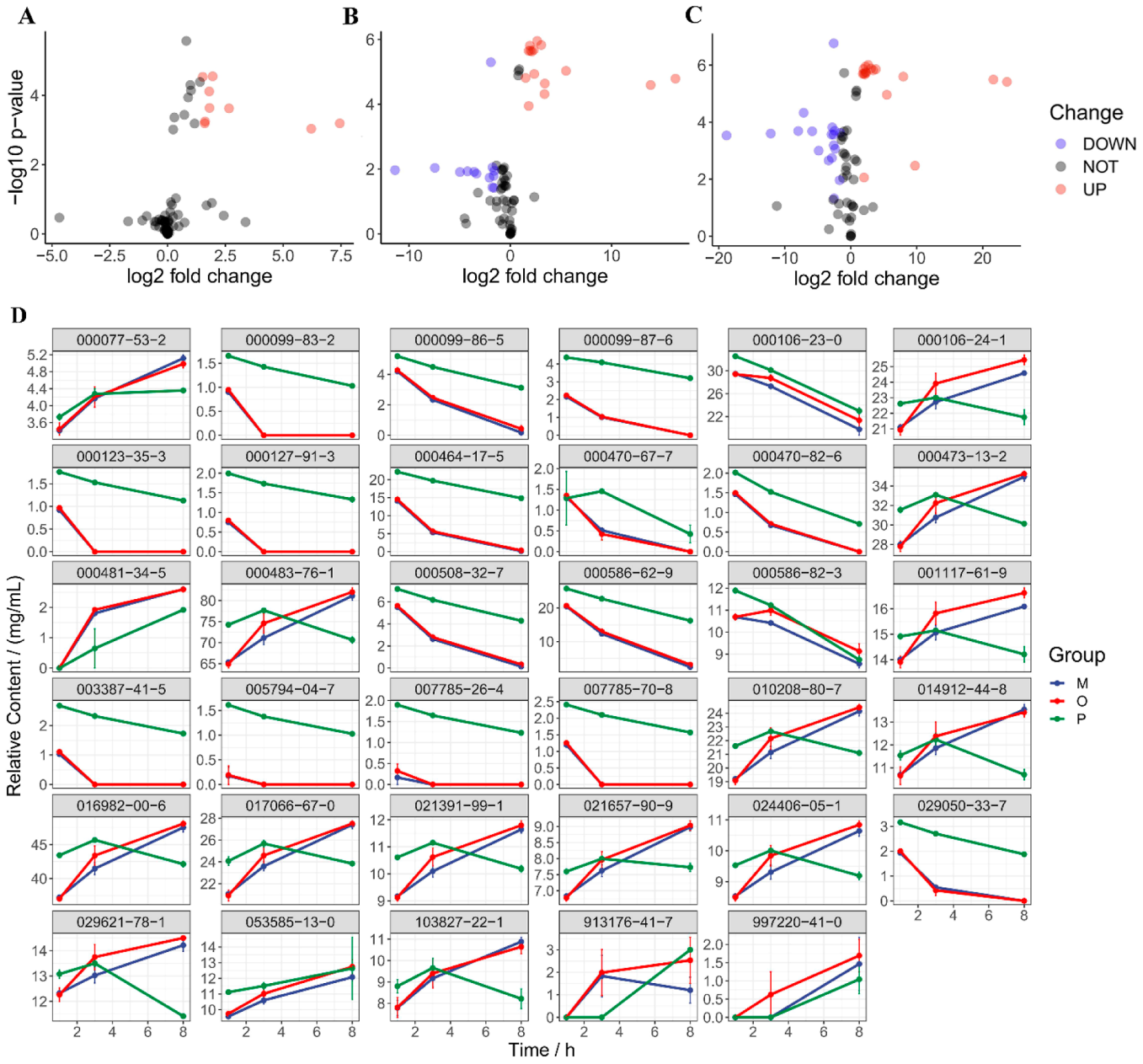

Figure 6. Screening of differential components and the line chart of differential components. Volcano plot of differential components between AT-EO without thermal treatment and AT-EO treated for 1 (A), 3 (B), and 8 h (C). (D) Line chart of differential components in the Pickering emulsion, physical mixture, and AT-EO.

The primary elements of amber were C (90.39%), O (4.32%), Al (0.12%), Si (0.29%), S (0.71%), and Ni (0.29%), and some elements have been previously reported in the related literature.[44] The main elements of PEG6000 were C (61.99%) and O (35.40%). The surface elements of modified amber particles consisted of C (88.18%), O (7.90%), S (0.32%), and Ni (0.26%), with no detection of Al and Si elements. Notably, the proportions of C, S, and Ni elements have decreased slightly, while the proportion of the O element has increased. The results of elemental analysis also successfully corroborated the encapsulation of PEG6000 on the surfaces of modified amber particles.

3.3. Single-Factor Investigation of Pickering Emulsion. *3.3.1. Added Amount of Modified Amber.* The added amount of modified amber was assessed using a comprehensive score (comprehensive scores = ESI/the maximum of ESI × 50% + postcentrifugation emulsion layer height/the maximum of postcentrifugation emulsion layer height × 50%). As depicted in Figure 3A, there is a progressive increase in the comprehensive score with an increasing quantity of modified amber added. A slow upward trend in the comprehensive score was observed when the amount of modified amber reached or exceeded 7.5 μg/mL. Additionally, it was noted that at lower additions of 2.5 and 5 μg/mL, the postcentrifugation emulsion layer was not adequately compact. Conversely, with a higher addition of 7.5 μg/mL and beyond, the emulsion layer was denser. Taking the principle of using excipient into consideration, the final amount of modified amber was determined to be 7.5 μg/mL.

3.3.2. Volume Fraction of AT-EO, Shear Rate, and Shear Time. The volume fraction of AT-EO, shear rate, and shear time were also evaluated using the comprehensive score. As

https://doi.org/10.1021/acsomega.3c08110
ACS Omega 2024, 9, 20773−20790

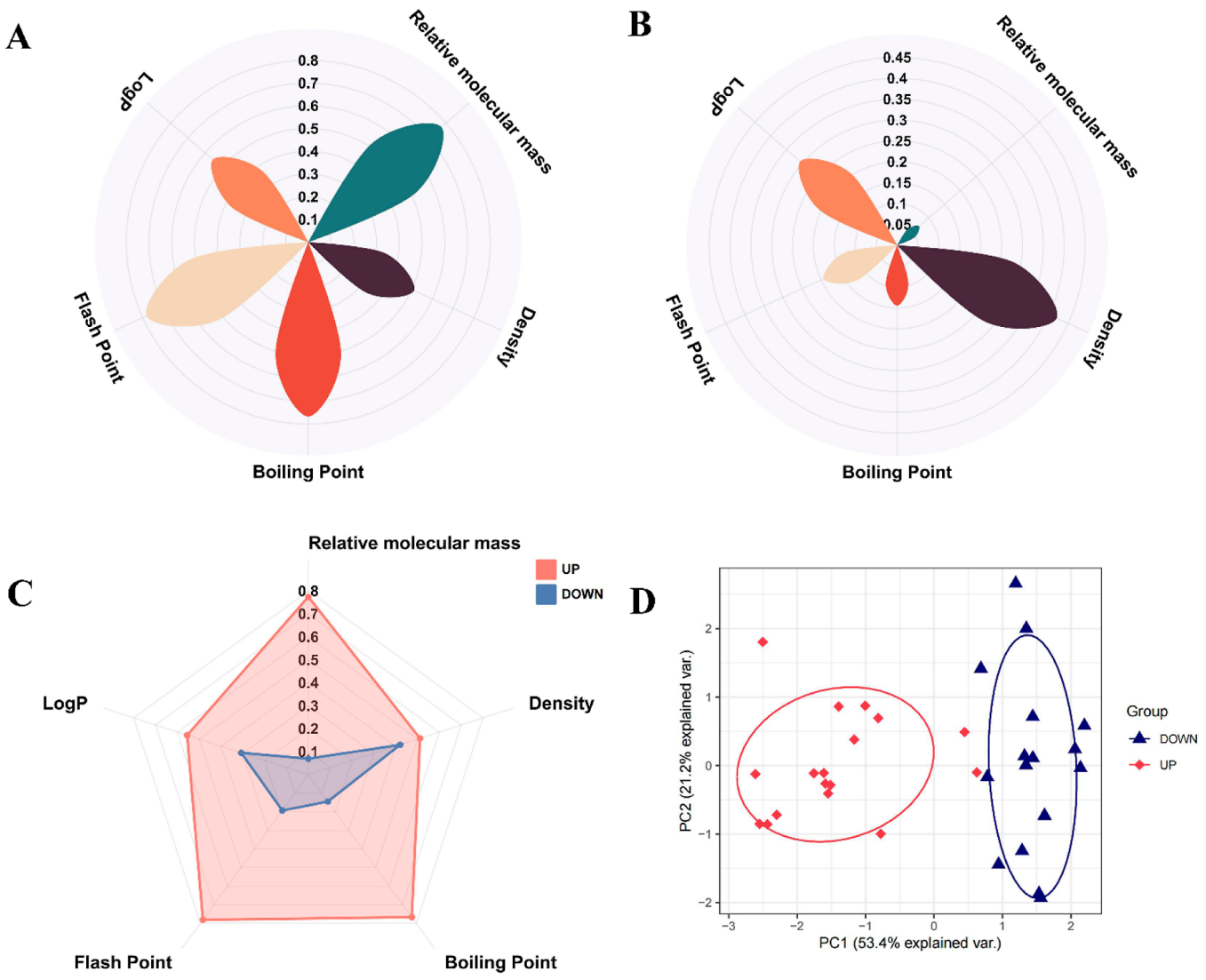

Figure 7. Differential component physicochemical property visualization suite. Flower petal plot of differential component physicochemical properties in the UP-regulation (A) and DOWN-regulation groups (B). Radar plot (C) and PCA plot (D) of differential component physicochemical properties in UP-regulation and DOWN-regulation groups.

was shown in Figure 3B, the optimal volume fraction for AT-EO was 65%. Furthermore, it was noted that at an AT-EO volume fraction of 80%, the Pickering emulsion stabilized with modified amber exhibited complex behavior, featuring a combination of W/O and O/W types of emulsions. When the volume fraction of AT-EO reached 85%, a complete transition to the W/O type of Pickering emulsion was observed. Based on the data presented in Figure 3C, the optimal shear rate was found to be 11,000 rpm. Figure 3D revealed that the optimal shear time was 2 min.

3.4. Characterization of Pickering Emulsion.

3.4.1. Emulsion Type. As depicted in Figure 3E,F, the external phase of the Pickering emulsion was dyed blue using methylene blue, while the internal phase of the Pickering emulsion was stained red with Sudan III. The microscopic staining results provided obvious confirmation that the Pickering emulsion, stabilized by modified amber, was an oil-in-water (O/W) type emulsion.

3.4.2. Droplet Size. The droplet size of the Pickering emulsion stabilized with modified amber was measured by a Microtrac S35000 laser particle size analyzer, and the results indicated a droplet size of 36.20 ± 0.77 μm.

3.4.3. Near Infrared Spectrum. The result in Figure 3G indicated the NIRS of Pickering emulsion stabilized by modified amber exhibited largely consistent with that of the suspension of modified amber. Only a weak characteristic peak of AT-EO was detected at 5000−6000 cm^{-1} in the NIRS of Pickering emulsion. This result strongly indicated that the modified ambers were coated on the outer layer of the AT-EO droplets within the Pickering emulsion.

3.4.4. Confocal Microscopy Analysis. The enclosure of AT-EO in the modified amber shell was confirmed with confocal microscope images (Figure 3H). AT-EO labeled with green fluorescence was observed inside the emulsion droplets, with Nile red distributed in the oil uniformly. Meanwhile, modified amber particles labeled with red fluorescence (Nile blue) were observed at the boundary of the emulsion droplets. The merge image clearly showed green oil droplets encapsulated by a red modified amber shell. These results suggested that the emulsion relied on the adsorption of solid particles at the oil−water interface. Furthermore, it also corroborated that the

https://doi.org/10.1021/acsomega.3c08110
ACS Omega 2024, 9, 20773−20790

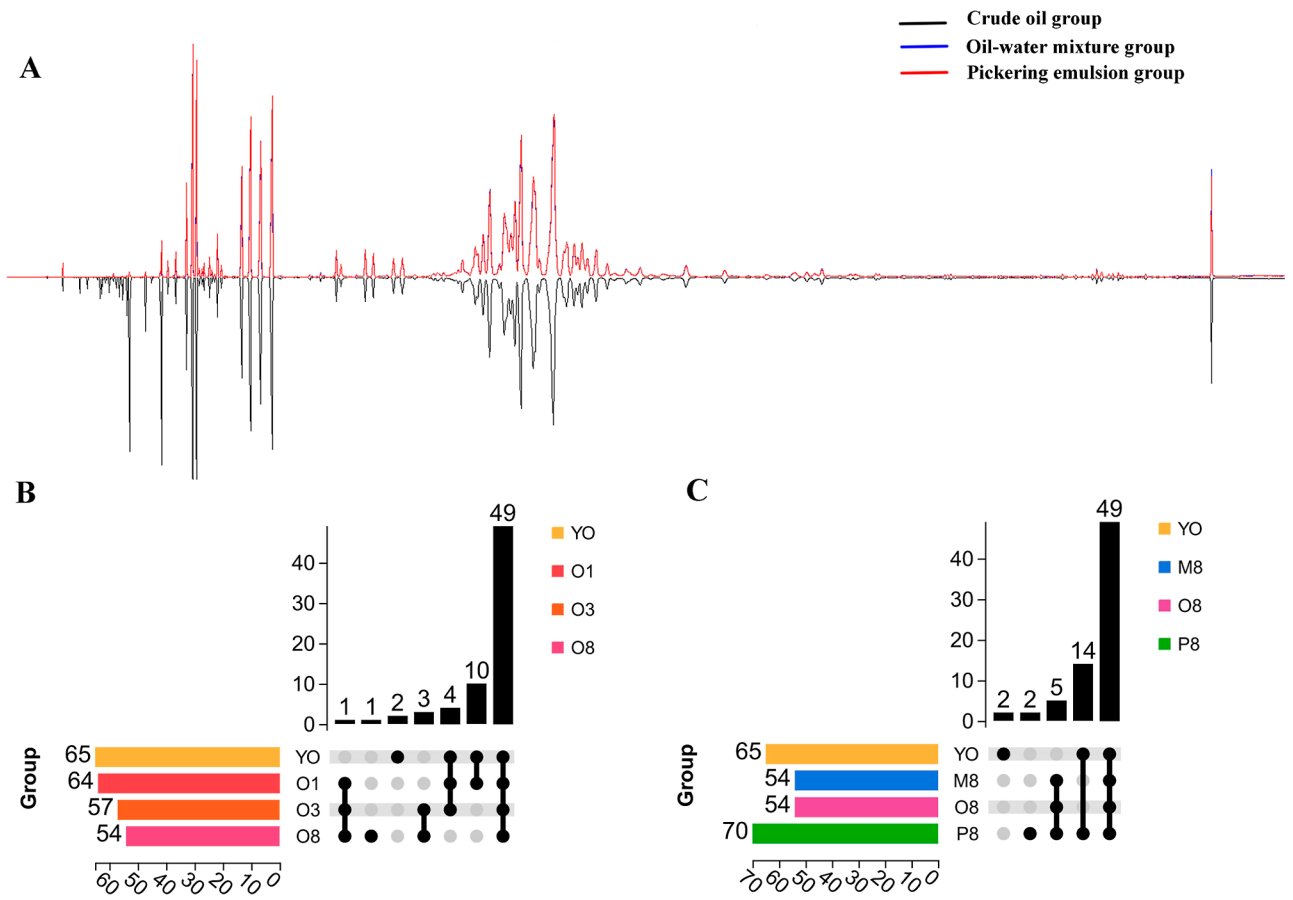

Figure 8. Screening of qualitative change components in AT-EO under heat treatment. (A) Stacked GC−MS chromatograms of Pickering emulsion, physical mixture, and AT-EO after 8 h of heat treatment. (B) Upset plot of the volatile components in AT-EO without thermal treatment and AT-EO after 1, 3, and 8 h of heat treatment. (C) Upset plot of the volatile components between AT-EO without thermal treatment and Pickering emulsion, physical mixture, and AT-EO groups after 8 h of heat treatment.

emulsion stabilized by modified amber particles was of the oil-in-water type.

3.5. Thermal Stability Studies of AT-EO in Each Group. *3.5.1. Overall Performance. 3.5.1.1. Retention Rate.* The retention rate of AT-EO reflects its volatilization rate in a thermal environment. As presented in Figure 4A, there was no significant difference observed in the retention rates of AT-EO among the three groups after 1 h of heat treatment, potentially due to the insufficient time of heat treatment to reveal the technologically superior preservation offered by Pickering emulsion. However, compared to the AT-EO group, the retention rates of AT-EO in Pickerign emulsion after 3 and 8 h were 83.08 ± 0.00 and 71.80 ± 0.89%, while the AT-EO group only had 77.13 ± 0.36 and 64.00 ± 1.23% of AT-EO remaining, and there was a significant difference ($P < 0.01$). The retention rate of AT-EO in the physical mixture group did not differ significantly from that of the AT-EO group. These results implied that Pickering emulsion stabilized by modified amber could substantially reduce its volatilization of AT-EO in a thermal environment.

3.5.1.2. Peroxide Value. After 1, 3, and 8 h of heat treatment, the PV of AT-EO in the Pickering emulsion group was 0.63 ± 0.05, 0.78 ± 0.03, and 1.03 ± 0.00 g/100 g, respectively, significantly lower than the PV in the AT-EO group ($P < 0.01$). Additionally, a noticeable difference in PV of AT-EO was also observed between the physical mixture and AT-EO groups after 3 and 8 h of heating ($P < 0.05$), of which the PV of the physical mixture group was 0.82 ± 0.03 and 1.08 ± 0.04 g/100 g, respectively. Notably, the AT-EO in Pickering emulsion exhibited lower PV than that in the physical mixture and AT-EO groups (Figure 4B). Pickering emulsion demonstrated a better protective effect on AT-EO, possibly due to the dense interface layer formed by the solid particles in Pickering emulsion, which acts as a barrier[45,46] to effectively mitigate the oxidation rate of AT-EO in the heating environment.

3.5.1.3. Malondialdehyde. The standard curve of MDA was as follows: $Y = 1.0797X\text{-}0.0042$ ($R^2 = 0.9993$), which was shown in Figure S1. The concentrations of MDA in the Pickering emulsion group after 1, 3, and 8 h of heat treatment, measured as 0.10 ± 0.01, 0.11 ± 0.01, and 0.12 ± 0.00 μg/mL, were significantly lower compared to those in the AT-EO group ($P < 0.01$). After 8 h of heat treatment, the MDA content of AT-EO in the physical mixture group was 0.16 ± 0.02 μg/mL, while it was 0.23 ± 0.04 μg/mL in the AT-EO group. There was a significant difference in the MDA content between the two groups ($P < 0.05$). Distinctly, the MDA content of AT-EO in the Pickering emulsion group was lower compared to both the physical mixture and AT-EO groups. As was shown in Figure 4C, these findings underscored the substantial efficacy of Pickering emulsion in preserving AT-EO, which was further confirmed by the lower MDA content in Pickering emulsion stabilized by modified cinnabaris.[47]

https://doi.org/10.1021/acsomega.3c08110
ACS Omega 2024, 9, 20773−20790

3.5.2. Changes in Content of Components. The total ion flow chromatogram of AT-EO, showing excellent separation, symmetric peak shapes, no overlap, and a smooth baseline, is depicted in Figure 5. Data Analysis and RStudio software were utilized to process the GC−MS data of each group, and a total of 72 kinds of volatile components were detected finally. The detailed information on these volatile components is shown in Table 3.

3.5.2.1. Screening of Differential Components. RStudio was employed to conduct differential component analysis by comparing the relative contents of volatile components between the AT-EO group subjected to 1, 3, and 8 h of heat treatment and untreated AT-EO, which was visualized through volcano plots. The screening criteria for differential components was Log2FC $\geq$ 1.5 and $P < 0.05$. As shown in Figure 6A−C, 9, 28, and 35 differential components were identified, respectively. After eliminated duplicates, a total of 35 differential components were finally obtained; they were (+)-cedrol (000077-53-2), geraniol (000106-24-1), (+)-δ-cadinene (000483-76-1), (*R*)-citronellol (001117-61-9), tricyclo [4.4.0.02,7] dec-3-ene, 1,3-dimethyl-8-(1-methylethyl)-, stereoisomer (014912-44-8), 1-methyl-4-[(1*R*)-1,2,2-trimethylcyclopentyl] benzene (016982-00-6), α-calacorene (021391-99-1), α-cadinene (024406-05-1), (4*E*)-1-methyl-4-(6-meth ylhept-5-en-2-ylidene) cyclohexene (053585-13-0), 4a,8-dimethyl-2-(prop-1-en-2-yl)-1,2,3,4,4a,5,6,7-octahydronaphthalene (103827-22-1), α-selinene (000473-13-2), (1*R*,4*S*,4aR,8aR)-4-isopropyl-1,6-dimethyl-1,2,3,4,4A,7,8,8A-octahydro-1-naphthalenol (000481-34-5), α-muurolene (010208-80-7), β-selinene (017066-67-0), hedycaryol (021657-90-9), 1-methyl-4-(1,2,2-trimethylcyclopentyl) cyclohexa-1,3-diene (029621-78-1), 4,8,11,11-tetramethylbicyclo [7.2.0] undec-3-en-5-ol (913176-41-7), italicene (997220-41-0), α-phellandrene (000099-83-2), *p*-cymene (000099-87-6), citronellal (000106-23-0), myrcene (000123-35-3), β-pinene (000127-91-3), cineole (000470-82-6), cyclene (000508-32-7), terpinolene (000586-62-9), 3-cyclohexen-1-ol,1-methyl-4-(1-methylethyl)-(000586-82-3), sabinene (003387-41-5), bicyclo [2.2.1] heptane (005794-04-7), (+)-4-carene (029050-33-7), α-terpinene (000099-86-5), 2-bornene (000464-17-5), 1,4-cineole (000470-67-7), (1*S*)-(−)-α-pinene (007785-26-4), and (1*R*)-(+)-α-pinene (007785-70-8).

3.5.2.2. Trends in teh Content of Differential Components. The changes in the relative content of the differential components across the three groups during the heat treatment process were further explored. As shown in Figure 6D, the relative content of certain differential components in the AT-EO and physical mixture groups exhibited an upward trend as the extended heat treatment time, such as 000077-53-2, 000106-24-1, 000473-13-2, 000481-34-5, 000483-76-1, 001117-61-9, 010208-80-7, 014912-44-8, 016982-00-6, 017066-67-0, 021391-99-1, 021657-90-9, 024406-05-1, 029621-78-1, 053585-13-0, 103827-22-1, and 997220-41-0. But, their tendency in the Pickering emulsion group was more stable. Moreover, the content of other components such as 000099-83-2, 000099-86-5, 000099-87-6, 00123-35-3, 000127-91-3, 000464-17-5, 000470-67-7, 000470-82-6, 000508-32-7, 000586-62-9, 003387-41-5, 005794-04-7, 007785-26-4, 007785-70-8, and 029050-33-7 steadily decreased as heat treatment progressed, with some components eventually diminishing to nondetectable levels. However, these components in the Pickering emulsion group exhibited a slower decline rate compared to the other two groups. The trend of fluctuation in content of 000106-23-0, 000586-82-3, and 913176-41-7 over heat treatment time was similar in the three groups, but their variation in Pickering emulsion was a little more intensive. In summary, Pickering emulsion demonstrated excellent protection for AT-EO by retarding the rate of volatility or the rise of most volatile components under heat treatment.

3.5.2.3. Predictive Analysis—the Factors Influencing Volatile Component Changes. By analysis of the content trend of 35 differential components in the AT-EO group during heat treatment, two main trends have been identified: the rising and falling trends with time. The physicochemical properties of the differential components, such as relative molecular mass, density, boiling point, flash point, and Log *P*, were investigated. For the differential components in the rising trend group (UP-regulation group) and the falling trend group (DOWN-regulation group), the values of its physicochemical parameters were normalized, and the average for each parameter were calculated, separately. As illustrated in Figure 7A,B, the relative molecular mass, boiling point, and flash point of differential components in the UP-regulation group were remarkable, while for those in the DOWN-regulation group had prominent density and Log *P*. Figure 7C provided a further comparison of the physicochemical property parameters between the two groups, revealing that the components in the UP-regulation group had higher relative molecular weight, boiling point, flash point, density, and Log *P* values compared with those in the DOWN-regulation group.

The PCA chart of the physicochemical properties of the differential components in the UP-regulation and DOWN-regulation groups exhibited a clear distinction (Figure 7D). PC1 and PC2 accounted for a cumulative variance contribution of 74.60%, suggesting that they were the main factors affecting the behavior of volatile component changes in the thermal environment. The components in the UP-regulation and DOWN-regulation groups were significantly distinguished along PC1. Specifically, PC1 = −0.58 × relative molecular mass −0.17 × density −0.56 × boiling point −0.38 × flash point −0.42 × Log *P*, with a variance contribution rate of 53.4%, of which relative molecular mass, density, boiling point, flash point, and Log *P* were negative correlation coefficient for PC1. It can be concluded from the above results that volatile components with lower relative molecular mass, boiling point, flash point, density, and Log *P* were more prone to volatilize. These results align with the research conducted by Farahbakhsh et al.,[48] a notable decrease in the content of low boiling point compounds during storage was observed. Meanwhile, a study on the volatilization rules of chemical components in volatile oil has demonstrated that components with small molecular weights show high volatilization curve slopes and fast volatilization speeds.[49] These results reveal that the physicochemical properties of volatile components indeed influence their behavior. Consequently, it is the necessity of dispositional attention to the physicochemical properties of volatile components in subsequent volatile oil stability work. Pickering emulsion stabilized by modified amber exhibited good essential oil stability by protecting AT-EO from external influences and reducing the impact of the physicochemical properties of the volatile components.

3.5.3. Changes in the Composition of Components. The stacked GC−MS chromatogram plot of Pickering emulsion, physical mixture, and AT-EO after 8 h of heat treatment

https://doi.org/10.1021/acsomega.3c08110
ACS Omega 2024, 9, 20773−20790

(Figure 8A) clearly exhibited distinct differences in the composition of volatile components among the three groups within the first 15 min. According to Figure 6D, some of the differential components gradually decreased to zero with increasing heat treatment time, while some components emerged as the heat treatment extended. The above findings revealed that qualitative changes occurred in some volatile components during the heat treatment process, resulting in transitions from present to absent or from absent to present. Therefore, it is necessary to further explore the protective role of Pickering emulsion technology on AT-EO from the perspective of qualitative changes.

The qualitative change components were identified by comparing the relative content using the Upset plot. Figure 8B revealed that 16 components in AT-EO disappeared with the prolongation of treatment time, while 5 new components were generated during the heat treatment process. Furthermore, the number of volatile components in AT-EO gradually decreased with a longer heat treatment duration. Figure 8C demonstrated that 16 components vanished in both the AT-EO and physical mixture groups after 8 h of heat treatment compared to the untreated AT-EO, whereas 14 of these components were retained in the Pickering emulsion. Additionally, there were 5 newly generated components shared by AT-EO, the physical mixture, and the Pickering emulsion, and 2 unique new components were found in the Pickering emulsion. These results imply that high temperatures significantly influence the composition of volatile components in AT-EO, primarily characterized by a trend of decreasing content and eventually leading to the disappearance of volatile components. Similar to the study conducted by Tai et al.,[36] the volatile components in turmeric essential oil underwent significant changes under prolonged high-temperature conditions, with a notable decrease in their content. However, the Pickering emulsion, stabilized by modified amber particles, effectively protects the volatile components in AT-EO from volatilization loss, thereby maintaining its original composition.

4. CONCLUSIONS

In this study, a hydrophilic modified amber was successfully prepared using the melt method with PEG6000 as a modifying agent. The modified amber was subsequently utilized to prepare an O/W-type Pickering emulsion for preserving AT-EO, which demonstrated an enhanced retention rate and reduced oxidation rate of AT-EO in high-temperature environments. Component analysis exhibited that high temperatures have a pronounced effect on the content and composition of AT-EO. The volatile components primarily exhibited a decreasing content trend, with certain components vanishing and becoming undetectable as time progressed. Pickering emulsion stabilized by modified amber effectively decelerated the volatilization of AT-EO in terms of both content and composition. Additionally, our analysis of the volatility rules of essential oils indicated that components with lower molecular mass, boiling point, flash point, density, and Log *P* are more prone to evaporation. In conclusion, the application of Pickering emulsion stabilized by a modified, suitable stabilizer contributes to the enhanced stability of AT-EO.

ASSOCIATED CONTENT

Supporting Information

The Supporting Information is available free of charge at https://pubs.acs.org/doi/10.1021/acsomega.3c08110.

Standard curve of malondialdehyde (PDF)

AUTHOR INFORMATION

Corresponding Authors

Junbo Zou − *Shaanxi Province Key Laboratory of New Drugs and Chinese Medicine Foundation Research, College of Pharmacy, Shaanxi University of Chinese Medicine, Xianyang 712046, China*; Email: 2051078@sntcm.edu.cn

Maomao Zhu − *China Pharmaceutical University, Nanjing 210009, China*; Email: 25666277@qq.com

Authors

Zhonghuan Qu − *Shaanxi Province Key Laboratory of New Drugs and Chinese Medicine Foundation Research, College of Pharmacy, Shaanxi University of Chinese Medicine, Xianyang 712046, China*; orcid.org/0009-0003-8948-8048

Yajun Shi − *Shaanxi Province Key Laboratory of New Drugs and Chinese Medicine Foundation Research, College of Pharmacy, Shaanxi University of Chinese Medicine, Xianyang 712046, China*

Xiaofei Zhang − *Shaanxi Province Key Laboratory of New Drugs and Chinese Medicine Foundation Research, College of Pharmacy, Shaanxi University of Chinese Medicine, Xianyang 712046, China*

Fei Luan − *Shaanxi Province Key Laboratory of New Drugs and Chinese Medicine Foundation Research, College of Pharmacy, Shaanxi University of Chinese Medicine, Xianyang 712046, China*

Dongyan Guo − *Shaanxi Province Key Laboratory of New Drugs and Chinese Medicine Foundation Research, College of Pharmacy, Shaanxi University of Chinese Medicine, Xianyang 712046, China*

Bingtao Zhai − *Shaanxi Province Key Laboratory of New Drugs and Chinese Medicine Foundation Research, College of Pharmacy, Shaanxi University of Chinese Medicine, Xianyang 712046, China*

Jing Sun − *Shaanxi Province Key Laboratory of New Drugs and Chinese Medicine Foundation Research, College of Pharmacy, Shaanxi University of Chinese Medicine, Xianyang 712046, China*

Dingkun Zhang − *College of Pharmacy, Chengdu University of Traditional Chinese Medicine, Chengdu 611137, China*; orcid.org/0000-0001-6746-3454

Complete contact information is available at: https://pubs.acs.org/10.1021/acsomega.3c08110

Author Contributions

Junbo Zou and Maomao Zhu designed this study and amended the final manuscript. Zhonghuan Qu performed the experiment and wrote the manuscript. Yajun Shi, Dingkun Zhang, Jing Sun, and Xiaofei Zhang provided technical help and did data analysis for this experiment. Dongyan Guo, Bingtao Zhai, and Fei Luan polished and revised the manuscript. All of the authors have read and approved the final manuscript.

https://doi.org/10.1021/acsomega.3c08110
ACS Omega 2024, 9, 20773−20790

Notes

During the preparation of this work, the authors used Dongdian AI in order to refinish and translate. After using this tool, the authors reviewed and edited the content as needed and take full responsibility for the content of the publication.

The authors declare no competing financial interest.

■ ACKNOWLEDGMENTS

This research was financially supported by the National Natural Science Foundation (no. 82274105, China), the Shaanxi Provincial Key Discipline of the Traditional Chinese Medicine and Pharmaceuticals Funding Project (no. 303061107, China), the Discipline Innovation Team Project of the Shaanxi University of Chinese Medicine (no. 2019-YL11, China), and the Shaanxi Province Key Subject of Pharmacy Engineering of the Shaanxi Provincial Traditional Chinese Medicine Administration (no. 2017001, China).

■ REFERENCES

(1) Luo, J.; Tian, X.; Liu, B.; Wang, C.; Li, L.; Yang, M. Application of essential oil components of aromatic Chinese materia medica in cardiovascular diseases. *Chin. Tradit. Herb. Drugs* **2020**, *51* (01), 245−255.

(2) Sanna, M. D.; Les, F.; Lopez, V.; Galeotti, N. Lavender (Lavandula angustifolia Mill.) Essential Oil Alleviates Neuropathic Pain in Mice With Spared Nerve Injury. *Front. Pharmacol* **2019**, *10*, 472.

(3) Zhang, L.; Yan, Q.; Zhang, W.; Li, X.; Zhang, X.; Du, S.; Hua, X.; Lin, J.; Shu, G.; Peng, G.; Tan, Z.; Fu, H. Enhancement of the functionality of attenuating acute lung injury by a microemulsion formulation with volatile oil of Angelicae Sinensis Radix and Ligusticum Chuanxiong Rhizoma encapsulated. *Biomed. Pharmacother.* **2022**, *156*, 113888.

(4) Huang, F.; Tong, X.; Hu, C.; Zhang, Q.; Wei, Y.; Hu, M.; Kong, L.; Fu, R.; Li, X.; Xie, Y.; Ming, X.; Chen, B.; Lin, Y.; Xiong, L.; Nadeem, S. CAVO Inhibits Airway Inflammation and ILC2s in OVA-Induced Murine Asthma Mice. *BioMed Res. Int.* **2023**, *2023*, 8783078.

(5) Mei, L.; Wang, F.; Yang, M.; Liu, Z.; Wang, L.; Chen, Q.; Li, F.; Zhang, X. Studies on the Mechanism of the Volatile Oils from Caoguo-4 Decoction in Regulating Spleen Deficiency Diarrhea by Adjusting Intestinal Microbiota. *Oxid. Med. Cell. Longevity* **2022**, *2022*, 5559151.

(6) Mancianti, F.; Ebani, V. V. Biological Activity of Essential Oils. *Molecules* **2020**, *25* (3), 678.

(7) Wu, Y.; Wan, N.; Liu, Y.; Lin, R.; Zhang, Y.; Guo, D.; Liao, J.; Zhou, T.; Wu, Z.; Yang, M. Influencing factors, changing mechanisms and protection strategies of volatile oil from traditional Chinese medicine. *Chin. Tradit. Herb. Drugs* **2022**, *53* (21), 6900−6908.

(8) Xing, L.; Li, H.; Wan, N.; Huang, X.; Yang, F.; Yang, M.; Wu, Z. Analysis on risk control of traditional Chinese medicine essential oil in clinical application. *Chin. Tradit. Herb. Drugs* **2021**, *52* (08), 2458−2464.

(9) Zhou, X.; Feng, L.; Zhang, X.; Yang, Y.; Jia, X.; Zou, J.; Shi, Y. Application of design technology for preparing Lingzhu Powder particles based on solvent evaporation method. *Oxid. Med. Cell. Longevity* **2021**, *46* (23), 6028−6034.

(10) Lin, Q.; Xu, M.; Cui, Z.; Pei, X.; Jiang, J.; Song, B. Structure and stabilization mechanism of diesel oil-in-water emulsions stabilized solely by either positively or negatively charged nanoparticles. *Colloids Surf., A* **2019**, *573*, 30−39.

(11) Lu, T.; Gou, H.; Rao, H.; Zhao, G. Recent progress in nanoclay-based Pickering emulsion and applications. *J. Environ. Chem. Eng.* **2021**, *9* (5), 105941.

(12) Gao, J.; Bu, X.; Zhou, S.; Wang, X.; Bilal, M.; Hassan, F. U.; Hassanzadeh, A.; Xie, G.; Chelgani, S. C. Pickering emulsion prepared by nano-silica particles - A comparative study for exploring the effect of various mechanical methods. *Ultrason. Sonochem.* **2022**, *83*, 105928.

(13) Chutia, H.; Mahanta, C. L. Properties of starch nanoparticle obtained by ultrasonication and high pressure homogenization for developing carotenoids-enriched powder and Pickering nanoemulsion. *Innovative Food Sci. Emerging Technol.* **2021**, *74*, 102822.

(14) Zhu, X.; Zhang, N.; Lin, W.; Tang, C. Freeze-thaw stability of pickering emulsions stabilized by soy and whey protein particles. *Food Hydrocolloids* **2017**, *69*, 173−184.

(15) Azfaralariff, A.; Fazial, F. F.; Sontanosamy, R. S.; Nazar, M. F.; Lazim, A. M. Food-grade particle stabilized pickering emulsion using modified sago (Metroxylon sagu) starch nanocrystal. *J. Food Eng.* **2020**, *280*, 109974.

(16) Wei, Y.; Niu, Z.; Wang, F.; Feng, K.; Zong, M.; Wu, H. A novel Pickering emulsion system as the carrier of tocopheryl acetate for its application in cosmetics. *Mater. Sci. Eng., C* **2020**, *109*, 110503.

(17) Yu, H.; Yue, P.; Huang, G.; Chen, Y.; Yang, M. Research Progress of Pickering Emulsion as a Drug Carrier. *China J. Pharm.* **2021**, *52* (6), 771−780.

(18) Yu, H.; Huang, G.; Ma, Y.; Liu, Y.; Huang, X.; Zheng, Q.; Yue, P.; Yang, M. Cellulose nanocrystals based clove oil Pickering emulsion for enhanced antibacterial activity. *Int. J. Biol. Macromol.* **2021**, *170*, 24−32.

(19) Zhang, D.; Fu, C.; Lin, J.; Ke, X.; Zou, W.; Xu, R.; Han, L.; Yang, M. Study on theory and application value of "unification of medicines and excipients" in Chinese materia medica preparations. *Chin. Tradit. Herb. Drugs* **2017**, *48* (10), 1921−1929.

(20) Gao, B.; Yuan, R.; Jin, Y.; Wang, L.; Wu, L.; Li, F.; Lin, Y. Effect of preparation process on the stability of volatile oil based on "unification of medicines and excipients. *Lishizhen Med. Mater. Med. Res.* **2018**, *29* (03), 609−610.

(21) Peng, L.; Feng, L.; Yang, Y.; liu, Y.; Zhang, X.; Zou, J.; Shi, Y. Improvement of thermal stability of Acorus tatarinowii volatile oil of pediatric drug Lingzhu Pulvis by Pickering emulsion technology based on concept of "combination of medicine and adjuvant. *Chin. Tradit. Herb. Drugs* **2023**, *54* (02), 544−552.

(22) Peng, L.; Zhang, X.; Guo, D.; Zhai, B.; Wang, M.; Zou, J.; Shi, Y. Pickering emulsion technology based on the concept of ″the combination of medicine and adjuvant″ to enhance the oxidation stability of volatile oils in solid preparations-taking Lingzhu Pulvis as an example. *RSC Adv.* **2022**, *12* (42), 27453−27462.

(23) Peng, L.; Wang, M.; Zhang, X.; Guo, D.; Zhai, B.; Zou, J.; Shi, Y. Research on Pickering emulsification technology based on the concept of "combination of medicine and adjuvant" to improve the pH stability of volatile oil in solid preparations—taking Lingzhu Pulvis as an Example. *AAPS Open* **2023**, *9* (1), 1.

(24) Yang, M.; Han, L.; Yang, S.; Zhang, D.; Su, Z.; Guo, Z.; Zou, W. Particles design technology for Chinese materia medica based on characteristics of traditional pill and powder. *Chin. Tradit. Herb. Drugs* **2012**, *43* (1), 9−14.

(25) Zou, J.; Feng, L.; Zhang, X.; Guo, D.; Shi, Y.; Jia, X. Application of particle design technology in field of traditional Chinese medicine powder. *Oxid. Med. Cell. Longevity* **2021**, *46* (23), 6011−6019.

(26) Chen, Q.; Zheng, J.; Xu, Y.; Yin, S.; Liu, F.; Tang, C. Surface modification improves fabrication of pickering high internal phase emulsions stabilized by cellulose nanocrystals. *Food Hydrocolloids* **2018**, *75*, 125−130.

(27) Ribeiro, A.; Manrique, Y. A.; Lopes, J. C. B.; Dias, M. M.; Barreiro, M. F. Development of water-in-oil Pickering emulsions from sodium oleate surface-modified nano-hydroxyapatite. *Surf. Interfaces* **2022**, *29*, 101759.

(28) Owens, D. K.; Wendt, R. C. Estimation of the Surface Free Energy of Polymers. *J. Appl. Polym. Sci.* **1969**, *13*, 1741−1747.

(29) Qin, C.; Han, L.; Zhang, D.; Guo, Z.; Wang, N.; Zhang, F. Effect of ultrafine grinding and powder modified on wettability and surface free energy of Indigo naturalis. *Chin. Tradit. Pat. Med.* **2013**, *35* (11), 2475−2479.

https://doi.org/10.1021/acsomega.3c08110
ACS Omega 2024, 9, 20773−20790

(30) Xi, X.; Wei, Z.; Xu, Y.; Xue, C. Clove Essential Oil Pickering Emulsions Stabilized with Lactoferrin/Fucoidan Complexes: Stability and Rheological Properties. *Polymers* **2023**, *15* (8), 1820.
(31) Chen, Z.-Z.; Yang, R.-P.; Shi, Y.-J.; Jia, X.-B.; Feng, L.; Guo, D.-Y.; Zhao, Z.-P. Powder modificationfor improving content uniformity of Ziyin Yiwei Capsules. *Oxid. Med. Cell. Longevity* **2021**, *46* (23), 6053−6061.
(32) Huang, Z.; Zhang, S.; Chang, J.; Liu, X. Preparation and in vitro dissolution determination of luteolin solid dispersion. *Chin. J. Hosp. Pharm.* **2023**, *43* (5), 494−500.
(33) Pearce, K. N.; Kinsella, J. E. Emulsifying properties of proteins: Evaluation of a turbidimetric technique. *J. Agric. Food Chem.* **1978**, *26* (3), 716−723.
(34) Agyare, K. K.; Addo, K.; Xiong, Y. L. Emulsifying and foaming properties of transglutaminase-treated wheat gluten hydrolysate as influenced by pH, temperature and salt. *Food Hydrocolloids* **2009**, *23*, 72−81.
(35) *GB 5009.227−2016. Determination of Peroxide Value in Food in National Food Safety Standards*; National Health and Family Planning Commission of the People's Republic of China: Beijing, 2016.
(36) Tai, J.; Zou, J.; Shi, Y.; Guo, D.; Zhang, X.; Liang, Y.; Li, J.; Cheng, J.; Yang, M.; Wang, Y.; Wang, F. Study on Stability of Volatile Oil in Foeniculi Fructus and Screening Its Antioxidants in Accelerated Oxidation Environment. *Chin. J. Exp. Tradit. Med. Formulae* **2019**, *25* (18), 108−115.
(37) *GB 5009.181−2016. Determination of Acetaldehyde in Food in National Food Safety Standards*; National Health and Family Planning Commission of the People's Republic of China: Beijing, 2016.
(38) Wickham, H.; FrançOis, R.; Henry, L.; Müller, K. *dplyr: A Grammar of Data Manipulation. R package* version 1.0.10, 2022 https://CRAN.R-project.org/package=dplyr.
(39) Ritchie, M. E.; Phipson, B.; Wu, D.; HuLaw, Y. C. W.; Shi, W.; Smyth, G. K.; Smyth, G. K. limma powers differential expression analyses for RNA-sequencing and microarray studies. *Nucleic Acids Res.* **2015**, *43* (7), No. e47-e47.
(40) Wickham, H. *ggplot2: Elegant Graphics for Data Analysis*; Springer Science & Business Media, 2016.
(41) Fang, L. *Pharmaceutics*; People's Medical Publishing House: Beijing, 2016.
(42) Ozbay, S.; Erbil, H. Y. Ice accretion by spraying supercooled droplets is not dependent on wettability and surface free energy of substrates. *Colloids Surf., A* **2016**, *504*, 210−218.
(43) Nakamura, M.; Hori, N.; Ando, H.; Namba, S.; Toyama, T.; Nishimiya, N.; Yamashita, K. Surface free energy predominates in cell adhesion to hydroxyapatite through wettability. *Mater. Sci. Eng., C* **2016**, *62*, 283−292.
(44) Huang, R.; Xing, Q.; Yu, L.; Zu, E. Organic components analysis of amber from different origins. *J. Guilin Univ. Technol.* **2017**, *37* (2), 280−284.
(45) Zhang, B.; Wang, Y.; Lu, R. Pickering emulsion stabilized by casein-caffeic acid covalent nanoparticles to enhance the bioavailability of curcumin in vitro and in vivo. *J. Sci. Food Agric.* **2023**, *103* (7), 3579−3591.
(46) Mwangi, W. W.; Lim, H. P.; Low, L. E.; Tey, B. T.; Chan, E. S. Food-grade Pickering emulsions for encapsulation and delivery of bioactives. *Trends Food Sci. Technol.* **2020**, *100*, 320−332.
(47) Ru, H.; Luan, F.; Shi, Y.; Zhang, X.; Guo, D.; Zhai, B.; Sun, J.; Zhang, D.; Zou, J. Cinnabaris modified with SiO2 nanoparticles stabilized Pickering emulsion to improve the photostability of volatile oil: A Lingzhu San case study. *Arabian J. Chem.* **2024**, *17* (1), 105442.
(48) Farahbakhsh, J.; Najafian, S.; Hosseinifarahi, M.; Gholipour, S. The effect of time and temperature on shelf life of essential oil composition of Teucrium polium L. *Nat. Prod. Res.* **2022**, *36* (1), 424−428.
(49) Ren, G.; Ke, G.; Huang, R.; Pu, Q.; Zhao, J.; Zheng, Q.; Yang, M. Study of the volatilization rules of volatile oil and the sustained-release effect of volatile oil solidified by porous starch. *Sci. Rep.* **2022**, *12* (1), 8153.

https://doi.org/10.1021/acsomega.3c08110
ACS Omega 2024, 9, 20773−20790